R. & M. No. 3218

MINISTRY OF AVIATION

AERONAUTICAL RESEARCH COUNCIL
REPORTS AND MEMORANDA

Effects of Heat Transfer on Laminar Boundary-Layer Development under Pressure Gradients in Compressible Flow

By R. J. MONAGHAN

LONDON: HER MAJESTY'S STATIONERY OFFICE
1961
PRICE: 15*s*. 0*d*. NET

Effects of Heat Transfer on Laminar Boundary-Layer Development under Pressure Gradients in Compressible Flow

By R. J. Monaghan

Communicated by the Deputy Controller Aircraft (Research and Development), Ministry of Aviation

*Reports and Memoranda No. 3218**
May, 1960

Summary. An approximate analysis, outlined in the Appendix, shows that momentum thickness, skin friction and heat transfer of the compressible laminar boundary layer developing under pressure gradients may be given by formulae formally the same as those obtaining under zero pressure gradient conditions if an appropriate length transformation is applied to the x-co-ordinate. Also, the formulae for skin friction and heat transfer include factors l and h respectively, which are functions of a pressure gradient parameter m.

Cohen and Reshotko's transformed similar solutions are used to provide values of $l(m)$ and $h(m)$ and of an index appearing in the length transformation. Compared with the pressure gradient parameter n of Cohen and Reshotko's generalised method, the present parameter $m = \frac{T_w}{T_0} n$ (where T_w is surface and T_0 is stagnation temperature), and there is a good collapse of values of l and h when plotted against m.

If pressure gradients are adverse, then the value of m at natural separation (which depends on T_w/T_0) is an additional parameter in the determination of the skin-friction parameter l, but h is approximately a constant, equal to its zero pressure gradient value, in this region.

Comparisons are made also for an external velocity variation $u_1 = u_a(1 - x)$.

1. *Introduction.* For a number of years, the so-called 'flat plate' (zero pressure gradient) formulae for estimating skin friction and heat transfer have enjoyed considerable popularity among the designers of high speed aircraft and missiles, largely because they are simple, concise and easy to apply. Also, the slender wings and bodies usually thought suitable for supersonic flight have involved only small pressure gradients (except, perhaps, in limited regions), so that a fair degree of accuracy could be expected. This expectation has been confirmed in many cases by comparison of theoretical predictions with experimental results.

Many refinements have been included in the formulae as the years progressed, but in their simplest form, assuming that viscosity (μ) varies linearly with temperature (T), we have

$$R_{\delta 2} = 0 \cdot 664 R_x^{1/2} \tag{1}$$

and

$$c_f R_x^{1/2} = 0 \cdot 664 \tag{2}$$

* Previously issued as R.A.E. Report Aero. 2640—A.R.C. 21,974.

for the momentum thickness and skin friction of zero pressure gradient, compressible, laminar boundary layers, where the local skin-friction coefficient

$$c_f = \frac{\tau_w}{\frac{1}{2}\rho_1 u_1^2}$$

and the Reynolds numbers

$$R_{\delta 2} = \frac{\rho_1 u_1 \delta_2}{\mu_1}$$

and

$$R_x = \frac{\rho_1 u_1 x}{\mu_1}$$

where τ_w is the local shearing stress at the wall,

δ_2 is momentum thickness $\left\{ = \int_0^\delta \frac{\rho u}{\rho_1 u_1}\left(1 - \frac{u}{u_1}\right) dy \right\}$

x, y are co-ordinates along and normal to the surface, respectively,

ρ is density,

u is the velocity component in the direction of x,

and suffix 1 denotes conditions in the stream outside the boundary layer.

A first approximation to the effects of pressure gradients, when the external velocity varies along the length of the body, is to use Equations (1) and (2) with ρ_1, u_1 and μ_1 taking their local, instead of their main-stream, values. This artifice is fairly successful if the velocity variations are small.

This is the situation in the (low) supersonic speed range. However, as speeds increase into the hypersonic regime, the need for protection against aerodynamic heating can lead to classes of shapes with relatively blunt leading edges (or noses) and appreciable variations in velocity along their length. An extreme example is the high drag-to-weight ratio body suitable for re-entry into the earth's atmosphere (*e.g.*, a sphere).

These trends lead to increased interest in methods for estimating boundary-layer development under appreciable pressure gradients. In particular there is interest in skin friction and heat transfer, and also in momentum thickness Reynolds number, which is of interest for predicting where transition to turbulence may occur. By contrast with similar studies in incompressible flow, there is little interest in predicting the natural separation point of a laminar boundary layer, since separation, if it occurs, is much more likely to be the result of a shock interaction.

The problem may be complicated by three-dimensional effects, interactions with the external flow and, indeed, the presence of shear in the external flow (caused by highly curved bow shock waves), so, in any treatment that neglects such effects (as in the present paper) there is much to be said for seeking simplicity in application, even if this sacrifices some accuracy. Approximate solutions using the momentum integral equation would seem to be suitable in this respect. Examples of such solutions are given by the work of Rott and Crabtree[1] and of Young[2] for cases with zero heat transfer, and of Cohen and Reshotko[3], and of Luxton and Young[4, 5] for the more general cases when heat is being transferred.

Effectively, these solutions of the momentum equation introduce a transformation of the x-co-ordinate which may be expressed in the form

$$X = \frac{\int_0^x \left(\frac{T_1}{T_a}\right)^{g\,2} u_1^{g\,1}\, dx}{\left(\frac{T_1}{T_a}\right)^{g\,2} u_1^{g\,1}} \tag{3}$$

where suffix a denotes a reference condition (from which local conditions are reached by an isentropic flow process), and g_1 and g_2 are functions for which various expressions are given by the various authors.

In the treatments by Luxton and Young[4, 5], g_1 and g_2 are quantities which vary with x, so that Equation (3) must be solved in step-by-step fashion. (However, in some of the cases they considered, quite large steps were adequate to give good agreement with known exact solutions.)

Concurrently with the later work of Luxton and Young[5], Monaghan and Crabtree made a similar study of the solution of the momentum integral equation (unpublished Royal Aircraft Establishment work). Starting from the same assumption, but with additional manipulation of the integral equation, they found it possible to obtain g_1 and g_2 as functions only of T_w/T_r (where T_r is recovery temperature), of viscosity-temperature relationship and of Prandtl number. An outline of this study is given in Appendix I. The result was what seemed to be a plausible extension of Thwaites' method[6] to compressible flow. For the case $\mu \propto T$ and Prandtl number unity, this gave

$$R_{\delta\,2} = 0\cdot664 R_X^{1/2} \tag{4}$$

$$c_f R_X^{1/2} = 0\cdot664 \left(\frac{l}{0\cdot22}\right) \tag{5}$$

where

$$R_X = \frac{\rho_1 u_1 X}{\mu_1}$$

with X given by Equation (3) with

$$\left.\begin{aligned} g_1 &= 3 + 2\frac{T_w}{T_0} \\ g_2 &= 2\cdot5 - \frac{T_w}{T_0} \end{aligned}\right\} \tag{6}$$

where T_0 is total temperature (invariant)
and T_w is wall temperature (assumed constant).

In Equation (5), l is a function of m, where

$$m = -\,0\cdot44\,\frac{T_w}{T_1}\frac{X}{u_1}\frac{du_1}{dx}\,. \tag{7}$$

The function $l(m)$ may be obtained from suitable correlations of known exact solutions (*e.g.*, in the first instance the correlation of incompressible flow results by Thwaites[6] was used). If pressure gradients are favourable, then the linear relation

$$l = 0\cdot22 - 1\cdot64m \tag{8a}$$

or

$$\frac{l}{0\cdot22} = 1 - 7\cdot45m \tag{8b}$$

may be adequate.

The similarity of Equations (4) and (5) to Equations (1) and (2) is apparent. The variations of the external flow quantities around the body will be known in advance, so the main source of additional work is the evaluation of X from Equation (3), with g_1 and g_2 from Equation (6).

Also, we may note that under zero heat transfer conditions, ($T_w = T_0$), g_1 and g_2 become the constants used by Rott and Crabtree[1].

If, instead of being given u_1, we are given the variation of Mach number M_1 around the body, then it is easily shown that Equations (3) and (7) become

$$X = \frac{\int_0^x \left(\frac{T_1}{T_a}\right)^4 M_1^{g_1}\, dx}{\left(\frac{T_1}{T_a}\right)^4 M_1^{g_1}} \tag{9}$$

and

$$m = -0{\cdot}44 \frac{T_w}{T_0} \frac{X}{M_1} \frac{dM_1}{dx} \tag{10}$$

with the remainder of the Equations staying as before.

Having obtained these results, comparisons were made with examples used by Luxton and Young[4,5] (the author wishes to acknowledge their co-operation in this respect), which showed deficiencies in some cases when heat was being transferred. These deficiencies are probably common to any method based on the very simple assumptions of the Appendix: in particular a straightforward transformation of Thwaites' incompressible flow correlation is not immediately possible. This was recognised by Luxton and Young in their modified method, wherein they introduced correction factors based on the transformed 'similar solutions' of Cohen and Reshotko[7].

This finding led to a critical examination of the formulae in relation to the transformed 'similar solutions'[7] which led to the conclusions to be discussed in the following sections. Section 2 considers the comparison with the similar solutions[7] and this is followed in Sections 3 and 4 with a fresh examination of the generalised approach[3] based on these similar solutions, which leads (Section 5) to what seems to be a sufficiently accurate method for estimating the development of compressible flow laminar boundary layers without sacrificing the simplicity of Equations (3) to (10) above.

2. *Comparison of the First Approximation with the Transformed Similar Solutions for $Pr = 1$ and $\mu \propto T$.* 2.1. *Results from Cohen and Reshotko*[7]. Application of the Stewartson-Illingworth transformations

$$\left.\begin{aligned} x_i &= \int_0^x \left(\frac{T_1}{T_0}\right)^4 dx \\ y_i &= \left(\frac{T_1}{T_0}\right)^{1/2} \int_0^y \frac{\rho}{\rho_0}\, dy \end{aligned}\right\} \tag{11}$$

reduces the differential equations of the laminar boundary layer to forms which, for $Pr = 1$, are

$$\left.\begin{aligned} &\frac{\partial u_i}{\partial x_i} + \frac{\partial v_i}{\partial y_i} = 0 \\ &u_i \frac{\partial u_i}{\partial x_i} + v_i \frac{\partial u_i}{\partial y_i} = \frac{H}{H_0} u_{i1} \frac{du_{i1}}{dx_i} + \nu_0 \frac{\partial^2 u_i}{\partial y_i^2} \\ &u_i \frac{\partial H}{\partial x_i} + v_i \frac{\partial H}{\partial y_i} = \nu_0 \frac{\partial^2 H}{\partial y_i^2} \end{aligned}\right\} \tag{12}$$

(where H is total enthalpy). These are identical with the corresponding equations of incompressible flow, except for a factor $\frac{H}{H_0}$ multiplying the velocity gradient term on the right-hand side of the momentum equation.

The transformed x-wise velocity, u_i, is

$$u_i = \frac{a_0}{a_1} u$$

and, for present purposes, we require only the velocity outside the boundary layer, so, in what follows, we shall take

$$\begin{aligned} u_i &= \frac{a_0}{a_1} u_1 \\ &= a_0 M_1 \,. \end{aligned} \tag{13}$$

If solutions in incompressible flow are known for an external velocity distribution $u_i = u_i\,(x_i)$, then when $T_w/T_0 = 1$ (zero heat transfer), we can transform the results by Equations (11) to obtain corresponding results for the distribution $M_1 = M_1(x)$ in compressible flow.

In particular the 'similar solutions' resulting from the velocity distributions

$$u_i = k x_i^{\overline{m}} \tag{14}$$

can be transformed in this manner.

This 1:1 correspondence does not hold when $T_w \neq T_0$, but, by a method of successive approximations, Cohen and Reshotko succeeded in obtaining transformed similar solutions for a range of T_w/T_0 from 0 to 2, and the numerical results are given in Ref. 7.

In particular they tabulate values of functions

$$\frac{\theta_{tr}}{x_i}\left(\frac{\overline{m}+1}{2}\frac{u_i x_i}{\nu_0}\right)^{1/2} = z \text{ (say)}$$

and

$$f_w'' = \tfrac{1}{2}\frac{T_0}{T_w} c_{f\,w}\left(\frac{2}{\overline{m}+1}\frac{\nu_0}{u_i x_i}\right)^{1/2}$$

(where $c_{f\,w} = \tau_w/\frac{1}{2}\rho_w u_1^2$ and $\theta_{tr} = (T_1/T_0)^3 \delta_2$ in the present notation).

With a small amount of manipulation we can transform these quantities to

$$\left(\frac{\overline{m}+1}{2}\frac{R_{\delta\,2}}{R_{x\,i}^{1/2}}\right)^{1/2}\left(\frac{T_1}{T_0}\right)^2 = z \tag{15}$$

and

$$\left(\frac{2}{\overline{m}+1}\right)^{1/2} \tfrac{1}{2} c_f R_{x\,i}^{1/2}\left(\frac{T_0}{T_1}\right)^2 = f_w'' \tag{16}$$

where

$$R_{\delta\,2} = \frac{\rho_1 u_1 \delta_2}{\mu_1}$$

and

$$R_{x\,i} = \frac{\rho_1 u_1 x_i}{\mu_1}\,.$$

2.2. *Results from the Present Method.* Turning now to the formulae of the present method, the appropriate length transformation is

$$X = \frac{\int_0^x \left(\frac{T_1}{T_0}\right)^4 M_1^{g_1} dx}{\left(\frac{T_1}{T_0}\right)^4 M_1^{g_1}} \tag{9}$$

with

$$g_1 = 3 + 2\frac{T_w}{T_0}. \tag{6}$$

Equation (9) includes the Stewartson-Illingworth transformation of the x-co-ordinate (note Equation (11)) and thus may be written

$$X = \frac{\int_0^{x_i} M_1^{g_1} dx_i}{\left(\frac{T_1}{T_0}\right)^4 M_1^{g_1}}. \tag{17}$$

Hence, with

$$u_i = a_0 M_1 = k x_i^{\overline{m}} \tag{14}$$

we obtain

$$\left(\frac{T_1}{T_0}\right)^4 X = \frac{x_i}{\overline{m}g_1 + 1} \tag{18}$$

and, from Equations (4), (5) and (7),

$$\begin{aligned} \left(\frac{\overline{m}+1}{2}\right)^{1/2} \frac{R_{\delta 2}}{R_{x\,i}^{1/2}} \left(\frac{T_1}{T_0}\right)^2 &= 0\cdot 664 \left(\frac{\overline{m}+1}{2(\overline{m}g_1+1)}\right)^{1/2} \\ &= 0\cdot 664\,\{2 + \beta_i(g_1 - 1)\}^{-1/2} \end{aligned} \tag{19}$$

where

$$\beta_i = \frac{2\overline{m}}{\overline{m}+1}$$

and

$$\begin{aligned} \left(\frac{2}{\overline{m}+1}\right)^{1/2} \tfrac{1}{2} c_f R_{x\,i}^{1/2} \left(\frac{T_0}{T_1}\right)^2 &= 0\cdot 332 \left(\frac{2(\overline{m}g_1+1)}{\overline{m}+1}\right)^{1/2} \left(\frac{l}{0\cdot 22}\right) \\ &= 0\cdot 332\,\{2 + \beta_i(g_1 - 1)\}^{1/2} \left(\frac{l}{0\cdot 22}\right) \end{aligned} \tag{20}$$

with l a function of

$$\begin{aligned} m &= -0\cdot 44 \frac{T_w}{T_0} \frac{\overline{m}}{\overline{m}g_1 + 1} \\ &= -0\cdot 44 \frac{T_w}{T_0} \frac{\beta_i}{2 + \beta_i(g_1 - 1)}. \end{aligned} \tag{21}$$

The right-hand sides of Equations (19) and (20) are to be compared with the tabulated values z and f_w'' of Equations (15) and (16). This is easily done over the whole range of values of β_i.

2.3. *Numerical Comparisons, on Basis of First Approximation for g_1 (Equation (6)).* Figs. 1 and 2 compare Cohen and Reshotko's values[7] of z and f_w'' with the approximations of Equations (19) and (20). In each case the plot is against β_i, where, as above,

$$\beta_i = \frac{2\bar{m}}{\bar{m}+1}.$$

Thus, $\beta_i < 0$ corresponds to adverse, and $\beta_i > 0$ to favourable pressure gradients. $\beta_i = 1$ corresponds to stagnation point flows and $\beta_i = 2$ to $\bar{m} = \infty$. The individual curves are for constant values of T_w/T_0. (Note the change in scale between $\beta_i > 0$ and $\beta_i < 0$.)

Considering the momentum thickness parameter z (Fig. 1), we see that the present approximation (Equation (19)) is reasonably accurate when pressure gradients are adverse. With favourable pressure gradients, there is good agreement when $T_w/T_0 = 1$ (zero heat transfer) but the approximation underestimates the spread of Cohen and Reshotko's results for other values of T_w/T_0. Effectively this means that Equation (6) for g_1,

$$g_1 = 3 + 2\frac{T_w}{T_0} \tag{6}$$

is not weighted sufficiently in favour of T_w/T_0 when pressure gradients are favourable.

The agreement for $T_w/T_0 = 1$ means that the sum of the numerical coefficients in Equation (6) should be around five. Alterations in the individual values (increasing the coefficient of T_w/T_0) would improve the approximation for $\beta_i > 0$, but immediately this would worsen the approximation for $\beta_i < 0$. Further consideration of g_1 will be deferred to Section 3.

Considering the skin-friction parameter f_w'' (in Fig. 2), where additional values of T_w/T_0 are included, we see that the present approximation is fairly reasonable over the whole range of β_i, except when approaching separation with negative β_i. (Note that the scale of f_w'' is altered between $\beta_i > 0$ and $\beta_i < 0$: that for $\beta_i < 0$ is the more open one.)

In estimating the function l of Equation (20), the linear approximation of Equation (8b)

$$\frac{l}{0\cdot 22} = 1 - 7\cdot 45m \tag{8b}$$

was used for $\beta_i > 0$. For $\beta_i < 0$, Thwaites' correlation[6] of the incompressible flow similar solutions were used.

However, if we use the revised values of $l\{= l(m, T_w/T_0)$ when $\beta_i < 0\}$ derived from Cohen and Reshotko[3] in Section 3 below, then the skin-friction results are in quite good agreement over the whole range of β_i. This is illustrated by the points (crosses) added for the case $T_w/T_0 = 0\cdot 2$ with $\beta_i < 0$. The reason for this agreement in skin-friction coefficients, whereas momentum thickness can be considerably in error, is that the errors in $R_{\delta 2}$ and m largely compensate for each other when estimating skin friction.

A feature of the approximate method is that when $T_w/T_0 = 0$, Equation (21) gives $m = 0$, so that $l = 0\cdot 22$ and the divergence of Equation (19) from the flat plate value of $0\cdot 332$ is accounted for solely by the X-transformation of Equations (17) and (18). This feature and the failure of Equation (6) for g_1 to give good results for momentum thickness over the whole range of β_i, led to a fresh examination, in Section 3 below, of Cohen and Reshotko's generalised method[3] for dealing with the laminar boundary layer in compressible flow.

3. *Examination of Cohen and Reshotko's Generalised Method*[3]. By analogy with Thwaites' treatment of incompressible flow, Cohen and Reshotko[3] introduce the correlation parameters

$$l = \frac{\theta_i}{u_{i1}} \left(\frac{\partial u_i}{\partial y_i}\right)_{y\,i=0}$$

and (23)

$$n = -\frac{\theta_i^2}{\nu_0} \frac{du_{i1}}{dx_i}$$

where $\theta_i\ (= \theta_{tr} \text{ of Ref. 7}) = \left(\frac{T_1}{T_0}\right)^3 \delta_2 .$

Then they draw on the transformed similar solutions of Ref. 7 to produce plots of the various boundary-layer functions against n. As an example of these plots, the skin-friction parameter l is plotted against n in Fig. 3 and shows considerable variation with T_w/T_0. (Note also the reversal of the curve for $T_w/T_0 = 2$ when $n < 0$.)

In the derivation of the present approximate method (Appendix I), Monaghan and Crabtree chose to define

$$\left.\begin{aligned} l &= \frac{\Delta_2}{u_1}\left(\frac{\partial u}{\partial Y}\right)_{Y=0} \\ m &= \frac{\Delta_2^2}{u_1}\left(\frac{\partial^2 u}{\partial Y^2}\right)_{Y=0} \end{aligned}\right\} \qquad (24)$$

(*i.e.*, *both* parameters are defined in terms of the derivatives, at the wall, of the velocity profile).

In Equations (24),

$$\Delta_2 = \frac{T_w}{T_1}\delta_2$$

$$Y = \int_0^y \frac{\mu_w}{\mu}\, dy$$

$$\left(= \int_0^y \frac{\rho}{\rho_w}\, dy \text{ if } \mu \propto T\right),$$

u is the velocity in the physical plane and, from the equations of motion with the aid of the Y-transformation,

$$\left(\frac{\partial^2 u}{\partial Y^2}\right)_{Y=0} = -\frac{\rho_1 u_1}{\mu_w}\frac{du_1}{dx}$$

(for more detail, *see* Appendix I).

Comparing Equations (23) and (24) (invoking the various transformations involved) it is easily shown that, in terms of quantities in the physical plane, the definitions of l are equivalent, but

$$m = \frac{T_w}{T_0} n . \qquad (25)$$

This suggested re-plotting Cohen and Reshotko's values of l against m, which has been done in Fig. 4. Compared with Fig. 3, there is a good collapse of the results for $m < 0$ (favourable pressure gradients). In particular the results for $0 \cdot 6 \leqslant T_w/T_0 \leqslant 2$* are close to the approximation of Equation (8a)

$$l = 0 \cdot 22 - 1 \cdot 64 m. \qquad (8a)$$

* Neglecting the reversal of the curve for $T_w/T_0 = 2$, shown by the broken (dashed) line.

For $m > 0$ (adverse pressure gradients) the curve for $T_w/T_0 = 1$ is the same as Thwaites' correlation of the similar solutions in incompressible flow (as would be expected), but there is a spread for other values of T_w/T_0. However, the individual curves exhibit a similarity in shape and those for $T_w/T_0 = 0 \cdot 2$ and $0 \cdot 6$ have been extrapolated to $l = 0$ in accordance with this similarity, instead of retaining the backward loops they had in Fig. 3. (The extrapolations commence from the breaks in the curves.)

Denoting the value of m for $l = 0$, by m_{sep} then Fig. 5a shows the values of m_{sep} (of Fig. 4) plotted against T_w/T_0, and Fig. 5b illustrates the similarity of shapes (for $m > 0$) by plotting l against m/m_{sep}. The individual points are derived from the numerical values of l and n tabulated by Cohen and Reshotko in Ref. 3.

Thus it is suggested that, when $m > 0$, the curve of l against m/m_{sep} of Fig. 5b be used to determine l; the value of m_{sep} being taken from Fig. 5a. (If the analysis is being made on the basis of the correlation of the similar solutions, then m_{sep} for $T_w = T_0$ is $0 \cdot 0681$.)

(In passing, it may be noted that the results for $m < 0$ do not correlate any better by plotting against m/m_{sep}. Instead, they are over-corrected and it seems preferable to use the simple plot of l against m when $m < 0$.)

Cohen and Reshotko also provide results for the case $T_w/T_0 = 0$, but a drawback of the present definition of m is that $m = 0$ when $T_w/T_0 = 0$, so they cannot be plotted on Fig. 4. $T_w/T_0 = 0$ is a limiting case and for practical purposes the drawback is obviated when $m > 0$ by using the alternative presentation of Fig. 5. When $m < 0$, one would expect the slopes of the curves for $T_w/T_0 < 0 \cdot 2$ (in Fig. 4) to increase more and more as T_w/T_0 tends to zero, finally becoming vertical when $T_w/T_0 = 0$. However, within the limits of the transformed similar solutions ($\beta_i \not> 2$) the deviation in the values of l would not be large. This is indicated by the dotted line which shows where the value $\beta_i = 2$ is reached on the curves for individual values of T_w/T_0.

In summary, therefore, it would seem that Equation (8a)

$$l = 0 \cdot 22 - 1 \cdot 64m$$

for $m < 0$ and Fig. 5 for $m > 0$, should provide reasonably accurate estimates of skin friction, provided m (or X, note Equations (7) and (10)) is estimated with sufficient accuracy. This question is considered in Section 4.

3.1. *Heat Transfer Coefficient.* Defining Stanton number

$$St = \frac{q_w}{\rho_1 u_1 c_p (T_0 - T_w)}$$

(where q_w is the heat flow per unit area and time), then, by analogy with Equation (5) for skin friction, we take

$$St R_X{}^{1/2} = 0 \cdot 332 \left(\frac{h}{0 \cdot 22} \right) \tag{25}$$

(remembering that the analysis is for Prandtl number unity).

Cohen and Reshotko's results[3] for skin friction and for the ratio of skin friction to heat transfer enable us to estimate h, and Fig. 6 plots h against m. The collapse of the results for the various values of T_w/T_0 is very good, apart from end-points, and, when pressure gradients are favourable ($m < 0$), a good approximation is given by

$$\left.\begin{aligned} h &= 0 \cdot 22 + 0 \cdot 6m \\ \text{or} \qquad \frac{h}{0 \cdot 22} &= 1 + 2 \cdot 7m\,. \end{aligned}\right\} \qquad (26)$$

This trend is the opposite to that displayed by $l(m)$.

An interesting feature when pressure gradients are adverse ($m > 0$) is that, unlike l, h does not tend to zero as separation is approached. There is a small decrease near to the separation point, but in general the values for $m > 0$ are nearly constant around $0 \cdot 220$ to $0 \cdot 225$.

4. *Improved Estimates of X and m.* To complete the solution, we require

$$X = \frac{\int_0^x \left(\frac{T_1}{T_a}\right)^4 M_1^{g_1}\, dx}{\left(\frac{T_1}{T_a}\right)^4 M_1^{g_1}} \qquad (9)$$

and

$$m = -\,0 \cdot 44 \frac{T_w}{T_0} \frac{X}{M_1} \frac{dM_1}{dx}\,. \qquad (10)$$

In Section 1, we took

$$g_1 = 3 + 2\frac{T_w}{T_0} \qquad (6)$$

which we shall refer to as the first approximation for g_1. We now seek improved values of g_1, which, in general, is a function of m as well as of T_w/T_0.

Equations (9) and (10), for X and m, have simple solutions (Equations (18) and (21)) for the transformed similar solutions, so we shall use Cohen and Reshotko's results[3,7] to find $g_1 = g_1(m, T_w/T_0)$. (Thus, from Equation (25) we have

$$m = \frac{T_w}{T_0} n \qquad (25)$$

and combined with Equation (21), this gives

$$g_1 = -\frac{0 \cdot 44 + \left(\frac{2 - \beta_i}{\beta_i}\right) n}{n}$$

and values of n are given in Ref. 3.)

The values of g_1 thus obtained are given in Table 1 and Figs. 7 to 9.

Concentrating first on the values of g_1 for $T_w/T_0 \leqslant 1$, Fig. 7 gives curves of g_1 against m for constant values of T_w/T_0. The full-line curves for $T_w/T_0 = 1$, $0 \cdot 6$ and $0 \cdot 2$ were obtained directly from the tabulated values of n in Ref. 3. The remainder were obtained by graphical interpolation*.

For $T_w/T_0 = 1$ (zero heat transfer), Fig. 7 shows that g_1 is approximately constant over the whole range of m. This feature would explain the success of Rott and Crabtree's solution of the

* Making use, in this interpolation, of the tabulated values[3] of n for $T_w/T_0 = 0$.

momentum equation for these conditions, using $g_1 = 5$ (note the agreement of results for $T_w/T_0 = 1$ in Figs. 1 and 2) and it would seem that a revised value of $g_1 = 4 \cdot 3$ to $4 \cdot 4$ would give very close agreement with the results of the transformed similar solutions.

However as T_w/T_0 is reduced below 1 (heat transfer from air to body), g_1 becomes increasingly dependent on m, so that, for close agreement at low values of T_w/T_0, a step-by-step integration of Equation (9), for X, would be necessary, changing the value of g_1 in accordance with the values of m obtained. (This feature has been noted already by Cohen and Reshotko[3].) In essence, this is the procedure adopted by Luxton and Young in their modified treatment[5].

However, it may still be possible to secure a good approximation to the exact results for momentum thickness, skin friction and heat transfer by choosing an overall mean value of g_1 for the range of values of m that may be expected in any particular problem. For example, when $m > 0$, the values of g_1 become grouped together and are in a region similar to that given by the first approximation (Equation (6)), although the actual values of g_1 vary by up to $0 \cdot 5$ from those given by the first approximation. This feature explains the success of the approximation in predicting momentum thickness parameter (Fig. 1) when $\beta_i < 0$ $(m > 0)$ and, in turn, the extent of the agreement found in Fig. 1 for $\beta_i < 0$ suggests that extreme accuracy in choosing g_1 is not essential.

An idea of the accuracy required is given by differentiating the momentum thickness parameter z (of Equations (15) and (19)) with respect to g_1, which gives

$$\left(\frac{dz}{z}\right) \Big/ \left(\frac{dg_1}{g_1}\right) = -\tfrac{1}{2} \frac{\beta_i g_1}{2 + \beta_i(g_1 - 1)} \, .$$

This shows that the maximum error in z is 50 per cent of the error in g_1. This occurs for $\beta_i = 2$. When $\beta_i = 1$, the error varies from 30 per cent for $g_1 = 1 \cdot 5$, to 40 per cent for $g_1 = 4 \cdot 5$.

Examples are given later. Meanwhile, Fig. 8 gives an alternative representation of the results for g_1, by plotting g_1 against T_w/T_0 for constant values of m. {The curve for $m = 0$ is a limiting case, dividing favourable $(m < 0)$ from adverse $(m > 0)$ pressure gradients.} This shows that, in most cases, a linear relation between g_1 and T_w/T_0 should be adequate. The relation varies from

$$g_1 \simeq 4 \cdot 25 \frac{T_w}{T_0} \qquad \text{when } m = -0 \cdot 1$$

through

$$g_1 \simeq 2 \cdot 3 + 2 \cdot 2 \frac{T_w}{T_0} \qquad \text{when } m = 0$$

to

$$g_1 \simeq 3 + 1 \cdot 5 \frac{T_w}{T_0} \qquad \text{when } m = 0 \cdot 02 \text{ to } 0 \cdot 04.$$

Finally, Fig. 9 gives g_1 against m for $T_w/T_0 = 2$. This shows the awkward feature that g_1 becomes double valued when $m < 0$, which is probably a characteristic of the similar solutions for all $T_w/T_0 > 1$. How this affects the application is considered in the examples of Section 6, but if there is an interest in problems with $T_w/T_0 > 1$ and favourable pressure gradients, then additional exact solutions of the boundary-layer equations for values of T_w/T_0 between 1 and 2 are essential.

5. *Suggested Method for Calculating the Development of the Laminar Boundary Layer for $Pr = 1$ and $\mu \propto T$.* The analysis of Sections 3 and 4 has shown that the method of calculation outlined in the Introduction should be adequate provided that suitable values of l and g_1 are used.

Recapitulating, the momentum thickness will be given by

$$R_{\delta 2} = 0\cdot 664 R_X^{1/2} \tag{4}$$

skin friction by

$$c_f R_X^{1/2} = 0\cdot 664 \left(\frac{l}{0\cdot 22}\right) \tag{5}$$

and heat transfer by

$$St R_X^{1/2} = 0\cdot 332 \left(\frac{h}{0\cdot 22}\right) \tag{25}$$

where Reynolds numbers and coefficients are based on local values of density, viscosity and velocity, outside the boundary layer and l (Figs. 4 and 5) and h (Fig. 6) are functions of m,

$$m = -0\cdot 44 \frac{T_w}{T_0} \frac{X}{M_1} \frac{dM_1}{dx} \tag{10}$$

which, for favourable pressure gradients ($m < 0$) may be approximated to by

$$\frac{l}{0\cdot 22} = 1 - 7\cdot 45 m \tag{8b}$$

and

$$\frac{h}{0\cdot 22} = 1 + 2\cdot 7 m \tag{26}$$

while, for adverse pressure gradients ($m > 0$), l is a function of T_w/T_0 as well as of m (but the dependence on T_w/T_0 may be removed by plotting against m/m_{sep}, where m_{sep}, the value of m at separation, varies with T_w/T_0; *see* Fig. 5), but h stays constant at approximately $0\cdot 225$.

For two-dimensional boundary layers (as considered so far), the transformed length co-ordinate X is given by

$$X = \frac{\int_0^x \left(\frac{T_1}{T_a}\right)^4 M_1^{g_1} dx}{\left(\frac{T_1}{T_a}\right)^4 M_1^{g_1}} \tag{9}$$

while, for bodies of revolution (as noted in Appendix I)

$$X = \frac{\int_0^x \left(\frac{T_1}{T_a}\right)^4 M_1^{g_1} r_0^2 dx}{\left(\frac{T_1}{T_a}\right)^4 M_1^{g_1} r_0^2} \tag{27}$$

where $r_0 = r_0(x)$ is the equation of the generating curve of the body.

The index g_1 is given in Figs. 7 and 8 as a function of T_w/T_0 and m. (Values of g_2, used in Equation (3), may easily be derived.)

In application, the starting values of m (at $x = 0$) should be easy to determine (from Equations (27) and (10), letting $x \to 0$). Then, knowledge of whether pressure gradients are favourable (m decreasing) or adverse (m increasing) should enable a suitable first approximation for g_1 (*i.e.*, a constant) to be chosen from Fig. 7 or Fig. 8. Using this approximation, Equation (9) (or (27)) is solved for X; hence m is obtained from Equation (10), whereupon reference back to Fig. 7 should indicate whether the first approximation is sufficient or whether a step-by-step integration, changing the value of g_1 with each step, is necessary. (The acid test comes from the values of $R_{\delta 2}$, which are affected most by changes in g_1.)

6. *Examples.* 6.1. *The Transformed Similar Solutions.* The comparisons in Figs. 1 and 2 have shown that the first approximation

$$g_1 = 3 + 2\frac{T_w}{T_0} \tag{6}$$

does not give good agreement for momentum thickness with Cohen and Reshotko's transformed similar solutions when pressure gradients are favourable ($m < 0$ or $\beta_i > 0$), except in the case $T_w/T_0 = 1$. Now, reference to Fig. 7 indicates that Equation (6) would hardly be considered to be a good first approximation when $T_w < T_0$ and $m < 0$. Thus, it is a fairly drastic test to go on to a second approximation on the basis of values of m determined from this clearly erroneous first approximation. This has been done and a new value of g_1 was determined for each value of β_i and T_w/T_0 *via* the first approximation to m and Fig. 7. The outline of the calculations is given in Table 2 for $T_w/T_0 = 0{\cdot}2$, and the results are plotted in Fig. 10 (momentum thickness) and Fig. 11 (skin friction). (Compared with Fig. 2, we have now used Fig. 5 for l when $m > 0$, with $(m_{\text{sep}})_{T_w = T_0} = 0{\cdot}0681$, whereas the corresponding region in Fig. 2 was based on Thwaites' correlation, which corresponds to the curve $T_w/T_0 = 1$ in Fig. 4.)

Fig. 10 shows that the second approximation for momentum thickness is within 10 per cent of the exact results over the whole range of β_i, for $0{\cdot}2 \leqslant T_w/T_0 \leqslant 1$. (The agreement would be better if a more reasonable first approximation had been taken.) On the whole, there is also better agreement between the skin-friction results (Fig. 11).

As mentioned in Section 4, there is a difficulty when $T_w/T_0 > 1$, since the $g_1(m)$ curve becomes double valued when $m < 0$ and extends only to $m = -0{\cdot}075$ (*see* Fig. 9). Therefore, in going to the second approximation, the last known value of g_1 on the lower part of the curve was used in cases when the first approximation to m lay beyond the limits of m in Fig. 9. Such values are enclosed by brackets in Table 2, for $T_w/T_0 = 2$.

The final results for $T_w/T_0 = 2$ in Table 2 and in Figs. 10 and 11 are in good agreement with the exact solutions until the point of departure from the lower curve for g_1 is reached (at $\beta_i = 0{\cdot}30$). After this, the values of the momentum thickness parameter (z, Fig. 10) show an increasing error. Surprisingly, the skin-friction parameter (f_w'', Fig. 11) remains in good agreement with the exact solutions up to the highest value of β_i used ($\beta_i = 1$). This arises from compensating errors in the factors $\{2 + \beta_i(g_1 - 1)\}^{1/2}$ and $l/0{\cdot}22$ (note Equation (20) and Table 2) and the same feature explains why the first approximation gave quite a good approximation to skin friction (in Fig. 2) in regions where its estimates of momentum thickness were considerably in error.

To improve on the approximation when $T_w/T_0 = 2$, and $\beta_i > 0{\cdot}3$, involves taking values of g_1 from the upper portion of the curve in Fig. 9, where it will be noted that g_1 varies rapidly with m. When the value m from the first approximation is greater negatively than $-0{\cdot}075$, then a suggestion would be to take the value of g_1 at its mirror image about $m = -0{\cdot}075$. In the present instance this would lead to an over-correction and the resulting values of z would come below the exact solution in Fig. 10 (for $\beta_i > 0{\cdot}3$). However, a third approximation might then be sufficient, but this was not checked.

6.2. *The External Velocity Distribution* $u_1 = u_a(1-x)$ *with* $M_a = 4$ *and* $T_w = T_a$. So far, the comparisons have all been with the transformed similar solutions, so it is useful to compare against results for a different type of external velocity distribution, as given by $u_1 = u_a(1-x)$.

A numerical solution has been obtained by the Mathematics Division of the National Physical Laboratory for the case $M_a = 4$ and $T_w = T_a$. This has been quoted to have an accuracy of about 10 per cent. Luxton and Young use it for a check on their modified method in Ref. 5 and the values to be used here are taken from that reference.

In applying the present method, the first approximation

$$g_1 = 3 + 2\frac{T_w}{T_0} = 3 \cdot 48 \quad (6)$$

was used, and the solution for X was obtained on MERCURY by Mr. A. Naysmith.

The results for skin friction and Reynolds number are given in Fig. 12, where it may be noted that the various quantities are based on the reference conditions 'a'.

Fig. 12 shows very close agreement between the present results for momentum thickness (δ_2) and those obtained by Luxton and Young (using their modified step-by-step method) until separation is approached.

The results for skin friction depend markedly on the assumption made about the value of m at separation (m_{sep}). In the first instance, the value of m_{sep} for $T_w = T_0$ was taken to be $0 \cdot 0681$, as for the similar solutions. In the case being considered, $T_w/T_0 = T_a/T_0 = 0 \cdot 24$, and Fig. 5a would give the appropriate m_{sep} to be $0 \cdot 034$. Fig. 12 shows that the resulting values of skin friction (using Fig. 5b for $l/0 \cdot 22$) are considerably below both the 'exact' solution and the results of Luxton and Young's modified method. Separation occurs at $x/L = 0 \cdot 175$ by the present method, at $0 \cdot 20$ by Luxton and Young and at $0 \cdot 22$ by the exact solution.

Now, from the variation of m with x/L obtained by the present method, $x/L = 0 \cdot 22$ corresponds to $m = 0 \cdot 042$, and by adopting this as the value of m_{sep} when estimating $l/0 \cdot 22$ from m/m_{sep} in Fig. 5b, the revised curve labelled '$m_{sep} = 0 \cdot 042$' was obtained, which shows quite good agreement with the exact solution.

The interesting feature is that this latter value of m_{sep} corresponds to an m_{sep} at $T_w = T_0$ (by Fig. 5a) of $0 \cdot 084$; while Thwaites' correlation[6] of Howarth's incompressible flow solution of $u_1 = u_a(1-x)$ gives $m_{sep} = 0 \cdot 082$.

The conclusion would be that agreement is obtained if the value of m_{sep} appropriate to the flow in question is used. Thus, although the position of natural separation may be only of academic interest in supersonic flows, it is still necessary to use it as a parameter when estimating skin friction under adverse pressure gradients. (However, it is not necessary to the evaluation of momentum thickness (δ_2), or Stanton number (St).)

For interest, the variations of $R_{\delta 2}/R_x^{1/2}$, $c_f R_x^{1/2}$ and $St R_x^{1/2}$, based on local conditions, are shown in Fig. 13. Results are included for $T_w = T_0$ as well as $T_w = T_a$ and the plot is against x/x_{sep}. (The value of x_{sep}/L for $T_w = T_0$, corresponding to $m_{sep} = 0 \cdot 084$, is $0 \cdot 063$.)

Comparing with the local flat-plate values (also shown) the variations of $R_{\delta 2}$ and St are larger for $T_w = T_a$ than for $T_w = T_0$, but both variations are small compared with those of c_f. (For $T_w = T_0$, the local flat-plate values would be good approximations to $R_{\delta 2}$ and St.) Also note that while $c_f R_x^{1/2}$ decreases with x/L, as would be expected with an adverse pressure gradient, the variation of $St R_x^{1/2}$ is in the opposite direction (*i.e.*, an increase).

7. *Concluding Remarks.* 7.1. *Skin Friction.* The results of the examples of Section 6 suggest that the method of calculation outlined in Section 5, and using a first approximation for g_1 (a constant, with value taken from Fig. 7 or 8) should be adequate for estimating skin friction, for $Pr = 1$ and $\mu \propto T$, particularly if pressure gradients are favourable ($m < 0$) and $T_w/T_0 < 1$. Similar accuracy with favourable pressure gradients, but $T_w/T_0 > 1$, would require additional exact solutions of the boundary-layer equations for T_w/T_0 between 1 and 2.

If pressure gradients are adverse ($m > 0$) then the accuracy depends primarily on knowledge of the value of m at natural separation, which is a parameter in the curve of l against m/m_{sep} of Fig. 5b. For external flows approximating to the transformed 'similar' flows $m_{sep} = 0 \cdot 068$ when $T_w = T_0$, but for flows of the type $u_1 = u_a(1-x)$, $m_{sep} = 0 \cdot 084$ when $T_w = T_0$ (from the example of Section 6.2).

7.2. *Momentum Thickness.* Compensating errors help to make the estimate of skin friction fairly independent of the accuracy of choice of g_1. However, the same is not true for momentum thickness, particularly if pressure gradients are favourable (and strong), and a second approximation, or a step-by-step integration of Equation (9), may be necessary. Experience would be the best guide in this respect and it is suggested that a second approximation should be made as a check in sample cases.

7.3. *Heat Transfer.* Estimates of heat transfer by Equations (25) and (26) have not been made, but the same remarks as for momentum thickness would apply when pressure gradients are favourable. It is of interest that when pressure gradients are adverse, the heat transfer parameter h (Fig. 6) does not vary appreciably with m, and a constant value of about $0 \cdot 225$ should be adequate.

7.4. *Extension to other Values of Pr and for more Realistic Variations of μ with T.* Approximate analyses of the type outlined in Appendix I may be of use for extending the results in these directions.

This suggests that a more realistic variation of μ with T may be allowed for by including a factor of the flat-plate intermediate-enthalpy type in the formulae for skin friction, etc., *e.g.*, Equation (5) would be replaced by

$$c_f R_X^{1/2} = 0 \cdot 664 C_1^{1/2} \frac{l}{0 \cdot 22}$$

where

$$C_1 = \frac{\rho_m \mu_m}{\rho_1 \mu_1}$$

the suffix m denoting that the quantity is to be evaluated at a reference (intermediate) enthalpy. Examples calculated by Luxton and Young would suggest that the assumption $\mu \propto T$ has negligible deleterious effect on the calculation of X.

Change in Prandtl number from 1 to $0 \cdot 72$ may have more effect and thus should be investigated further. Until this is done, a first approximation would be to use the equations for momentum thickness and skin friction as they stand, but to modify the equation for heat transfer (Equation (26)) by the inclusion of a factor depending on Prandtl number, *e.g.*,

$$St R_X^{1/2} = 0 \cdot 332 Pr^{-\alpha} \left(\frac{h}{0 \cdot 22}\right)$$

(and include also the factor $C_1^{1/2}$) where, from Cohen and Reshotko[3], following Tifford and Chu[8], and Squire[9]

$$\alpha = 0\cdot667 \text{ for small pressure gradients}$$

$$\alpha = 0\cdot6 \quad \text{for stagnation point flows}^9$$

$$\alpha = 0\cdot5 \quad \text{for extreme favourable gradients}^8$$

$$\text{and } \alpha = 0\cdot75 \quad \text{for large adverse gradients}^8.$$

Likewise, one would take a recovery factor (say $= Pr^{1/2}$) when estimating recovery (zero heat transfer) temperature, and the various curves for constant values of T_w/T_0 should be read as for T_w/T_r, where T_r is the recovery temperature.

NOTATION

A, B	Functions of Prandtl number defined in Equation (31) of Appendix I
C	Constant in the viscosity-temperature relation (Equations (38) of Appendix I)
$\mathscr{H}$	Shape factor, δ_1/δ_2
H	Total enthalpy
M	Mach number
Pr	Prandtl number ($= c_p\mu/k$, where k is thermal conductivity)
R	Reynolds number $\left(R_x = \dfrac{\rho_1 u_1 x}{\mu_1}, \text{etc.}\right)$
St	$= \dfrac{q_w}{\rho_1 u_1 c_p (T_r - T_w)}$ Stanton number (heat transfer coefficient)
T	Temperature
X	Transformed length co-ordinate, along surface of body, defined by Equation (3) (or (9))
Y	Transformed distance normal to the surface, using Howarth transformation (Equation (30) of Appendix I)
a	Speed of sound
c_p	Specific heat at constant pressure
c_f	Local skin-friction coefficient ($= \tau_w/\frac{1}{2}\rho_1 u_1^2$)
f_w''	Skin-friction parameter used by Cohen and Reshotko (Equation (16))
f_1, f_2	Constants defined in Equation (42) of Appendix I
g_1, g_2	Indices in the X-transformation (Equation (3) or (9))
h	Factor in Equation (25) for Stanton number (a function of m, Equation (26))
l	Factor in Equation (5) for skin-friction coefficient (defined by Equation (24); a function of m)
m	Pressure-gradient parameter (*see* Equations (24), (7) and (10))
m_{sep}	Value of m at natural separation point of laminar boundary layer
$\overline{m}$	Index of the 'similar' flows ($u_i \propto x^{\overline{m}}$)
n	pressure gradient parameter used by Cohen and Reshotko[3]. $\left(m = \dfrac{T_w}{T_0} n\right)$
p	Pressure
q_w	Heat flow rate per unit area *into* surface of body
u, v	Components of velocity in the directions x and y
x, y	Co-ordinates along and normal to the surface of the body

x_i, y_i		Co-ordinates along and normal to the surface of the body, following the Stewartson-Illingworth transformations (Equation (11))
z		Momentum-thickness parameter of Equation (15)
β_i	=	$2\overline{m}/(\overline{m}+1)$
δ		Thickness of boundary layer
δ_1, δ_2		Displacement and momentum thicknesses of boundary layer
Δ_2		Momentum thickness in the (x, Y) plane
μ		Viscosity
ρ		Density
τ		Local shear stress

SUFFIXES
(to velocity, temperature, etc.)

w	At wall (body surface)
1	Locally in the stream outside the boundary layer
0	Stagnation (isentropic)
a	Reference (isentropic)
r	Recovery (zero heat transfer)
i	Incompressible, following the Stewartson-Illingworth transformations

Editor's note. To simplify the casting of the mathematics by machine a suffix, or power, with an inferior suffix attached has been printed with the inferior on line, but detached by a thin space.

REFERENCES

No.	Author	Title, etc.
1	N. Rott and L. F. Crabtree ..	Simplified laminar boundary-layer calculations for bodies of revolution and for yawed wings. *J. Ae. Sci.* Vol. 19. No. 8. pp. 553–565. August, 1952.
2	A. D. Young	Skin friction in the laminar boundary layer in compressible flow. *Aero. Quart.* Vol. 1. pp. 137–164. August, 1949.
3	C. B. Cohen and E. Reshotko ..	The compressible laminar boundary layer with heat transfer and arbitrary pressure gradient. N.A.C.A. Report 1294. 1956.
4	R. E. Luxton and A. D. Young ..	Skin friction in the compressible laminar boundary layer with heat transfer and pressure gradient. Queen Mary College, University of London. A.R.C. 20,336. July, 1958.
5	R. E. Luxton and A. D. Young ..	A generalised method for the calculation of the laminar compressible boundary layer with heat transfer and non-uniform pressure distribution. Queen Mary College, University of London. R. & M. 3233. January, 1959.
6	B. Thwaites	Approximate calculation of the laminar boundary layer. *Aero. Quart.* Vol. 1. Part III. pp. 245–280. November, 1949.
7	C. B. Cohen and E. Reshotko ..	Similar solutions for the compressible laminar boundary layer with heat transfer and pressure gradient. N.A.C.A. Report 1293. 1956.
8	A. N. Tifford and S. T. Chu ..	Heat transfer in laminar boundary layers subject to surface pressure and temperature distributions. Proc. 2nd Midwestern Conf. on Fluid Mechanics. pp. 363–377. Ohio State Univ. March, 1952.
9	.. ..	*Modern developments in fluid dynamics.* Vol. 2. Chap. 14. pp. 631–632. Clarendon Press, Oxford. 1938.
10	R. J. Monaghan	On the behaviour of boundary layers at supersonic speeds. Proc. 5th Anglo-American Aeronautical Conference, Los Angeles. June, 1955.

(82477) B*

APPENDIX I

Outline of an Approximate Method of Solution of the Momentum Integral Equation, for C_P = Constant

The momentum integral equation of the steady, two-dimensional laminar boundary layer in compressible flow is

$$\frac{d\delta_2}{dx} + \delta_2 (\mathscr{H}+2)\frac{1}{u_1}\frac{du_1}{dx} + \delta_2 \frac{1}{\rho_1}\frac{d\rho_1}{dx} = \tfrac{1}{2}c_f \tag{28}$$

where δ_2 is momentum thickness $\left\{ = \int_0^\delta \frac{\rho u}{\rho_1 u_1}\left(1 - \frac{u}{u_1}\right) dy \right\}$

$\mathscr{H} = \frac{\delta_1}{\delta_2}$ is the shape factor

δ_1 is displacement thickness $\left\{ = \int_0^\delta \left(1 - \frac{\rho u}{\rho_1 u_1}\right) dy \right\}$

and $c_f = \frac{\tau_w}{\frac{1}{2}\rho_1 {u_1}^2}$ is the local skin-friction coefficient, based on local conditions in the stream outside the boundary layer.

(For other symbols, *see* Notation.)

In any given problem, the variations of stream density (ρ_1) and stream velocity (u_1) with x will be known, and to solve Equation (28) for δ_2 we need to insert in it suitable expressions for $\mathscr{H}$ and c_f.

The solution is aided by the conditions

$$-\rho_1 u_1 \frac{du_1}{dx} = \frac{dp}{dx}$$

$$= \left\{ \frac{\partial}{\partial y}\left(\mu \frac{\partial u}{\partial y}\right) \right\}_{y=0} \tag{29}$$

which are obtained from the momentum equation in its standard differential form, where p is pressure and μ is viscosity.

1. *Transformation of the y-Co-ordinate.* *We assume* that if the co-ordinate normal to the surface (y) is replaced by Y, using the transformation

$$Y = \int_0^y \frac{\mu_w}{\mu} dy \tag{30}$$

then the velocity profile $u = u(Y)$ is not affected by compressibility. In essentials this is the transformation used by Luxton and Young[4, 5] and it is closely related to Howarth transformation. The assumption that $u(Y)$ is not affected by compressibility is certainly valid if $\mu \propto T$ and $dp/dx = 0$, since in this case there is a unique curve of τ/τ_w against u/u_1 for all values of M_1 and T_w/T_1 (where τ is the shearing stress locally within the boundary layer). We now assume that it may also be a reasonable approximation when $dp/dx \neq 0$.

2. *Value of the Shape Factor $\mathscr{H}$.* In general, the shape factor $\mathscr{H}$ is a function of Mach number, of surface temperature and of the history of the boundary layer. The problem is simplified if $dp/dx = 0$ (the 'flat plate' boundary layer) in which case $\mathscr{H}$ is given, to very good approximation[10], by

$$\mathscr{H} = \mathscr{H}_i + A\mathscr{H}_i\left(\frac{T_w}{T_1} - 1\right) + B\left(\frac{T_r}{T_1} - 1\right) \tag{31}$$

where T_1, T_w and T_r are the 'static' (outside boundary layer), wall and recovery temperatures and A, B are functions of Prandtl number, with numerical values as given below.

$Pr =$	0·65	0·70	0·72	0·75	1·0
$A =$	1·23	1·20	1·18	1·16	1
$B =$	1·07	1·03	1·05	1·04	1

We may note that if $Pr = 1$ then $A = B = 1$ so that

$$\mathscr{H} = \mathscr{H}_i \frac{T_w}{T_1} + \left(\frac{T_r}{T_1} - 1\right) \tag{31a}$$

as has been used by several authors.

In deriving Equation (31), it was assumed that total enthalpy was a linear function of velocity (in the boundary layer) and this is not always a good approximation if $dp/dx \neq 0$. However, we shall assume that Equation (31) can be used in the present case if a suitable mean value for $\mathscr{H}_i$ is chosen.

Meanwhile it is convenient to re-write Equation (31) in a form that isolates the quantities that vary along the length of the body from those that are constant (or nearly constant). T_w/T_r will be assumed constant, but T_1 can vary considerably, so we replace T_w/T_1 by

$$\begin{aligned}\frac{T_w}{T_1} &= \frac{T_w}{T_r}\frac{T_r}{T_1} \\ &= \frac{T_w}{T_r} + \frac{T_w}{T_r}\left(\frac{T_r}{T_1} - 1\right)\end{aligned} \tag{32}$$

and Equation (31) becomes

$$\mathscr{H} = \mathscr{H}_i + A\mathscr{H}_i\left(\frac{T_w}{T_r} - 1\right) + \left(A\mathscr{H}_i\frac{T_w}{T_r} + B\right)\left(\frac{T_r}{T_1} - 1\right). \tag{33a}$$

In application, we shall then assume that

$$\frac{T_r}{T_1} - 1 = Pr^{1/2}\frac{\gamma - 1}{2}M_1^2 \tag{34}$$

hence

$$\mathscr{H} = \mathscr{H}_i + A\mathscr{H}_i\left(\frac{T_w}{T_r} - 1\right) + Pr^{1/2}\left(A\mathscr{H}_i\frac{T_w}{T_r} + B\right)\frac{\gamma - 1}{2}M_1^2 \tag{33b}$$

3. *Relation between c_f, δ_2 and du_1/dx.* We have assumed that the velocity profile $u(Y)$ is not affected by compressibility where

$$Y = \int_0^y \frac{\mu_w}{\mu}\,dy\,. \tag{30}$$

The outer edge of the boundary layer, $y = \delta$ corresponds to $Y = \Delta$ where

$$\Delta = \int_0^\delta \frac{\mu_w}{\mu}\, dy$$

and $u = u(Y)$ must satisfy the boundary conditions

$$\left.\begin{aligned} Y &= \Delta; \qquad u = u_1, \qquad \frac{\partial u}{\partial Y} = \frac{\partial^2 u}{\partial Y^2} = 0 \\ Y &= 0; \qquad u = 0, \qquad T = T_w \end{aligned}\right\} \tag{35}$$

A further condition is given by Equation (29), which is transformed by Equation (30) to give

$$\left(\frac{\partial^2 u}{\partial Y^2}\right)_{Y=0} = -\frac{\rho_1 u_1}{\mu_w}\frac{du_1}{dx}\,. \tag{36}$$

Equations (35), (36) are the usual boundary conditions of incompressible flow (note, however, the combination of ρ_1 and μ_w in (36)) and we shall assume that we can make use of known solutions to obtain c_f as a function of Δ_2 and du_1/dx, where

$$\begin{aligned} \Delta_2 &= \int_0^\Delta \frac{u}{u_1}\left(1 - \frac{u}{u_1}\right) dY \\ &= \frac{1}{C_w}\frac{\rho_1}{\rho_w}\,\delta_2 \end{aligned} \tag{37}$$

C_w being an appropriately chosen constant in the approximate viscosity-temperature relation

$$\frac{\mu}{\mu_w} = C_w \frac{T}{T_w}\,. \tag{38}$$

Thus

$$C_w \simeq \frac{\mu T_w}{\mu_w T} = \frac{\rho\mu}{\rho_w \mu_w}$$

and in the case $dp/dx = 0$ we would take

$$C_w = \frac{\rho^* \mu^*}{\rho_w \mu_w} \tag{38a}$$

where the asterisks denote that quantities are to be evaluated at 'intermediate' enthalpy. We shall also use

$$C_1 = \frac{\rho^* \mu^*}{\rho_1 \mu_1}\,. \tag{38b}$$

3.1. *Use of Thwaites Correlation.* Thwaites[6] characterises known solutions of the incompressible boundary-layer equations in terms of momentum thickness and of the first and second derivatives (at the wall) of the velocity profile, setting

$$\left.\begin{aligned} \left(\frac{\partial u}{\partial Y}\right)_{Y=0} &= \frac{u_1}{\Delta_2}\, l \\ \left(\frac{\partial^2 u}{\partial Y^2}\right)_{Y=0} &= \frac{u_1}{\Delta_2^2}\, m\,. \end{aligned}\right\} \tag{39}$$

From these, using Equations (30) and (37) we obtain

$$\tfrac{1}{2}c_f = \frac{\tau_w}{\rho_1 u_1^2} = C_w \frac{\rho_w}{\rho_1} \frac{u_w l}{\rho_1 u_1 \delta_2} \tag{40a}$$

or

$$c_f R_{\delta 2} = 2C_1 l \tag{40b}$$

(with C_1 from Equation (38b)

where $R_{\delta 2} = \dfrac{\rho_1 u_1 \delta_2}{\mu_1}$ is a *local* Reynolds number.

Also, l is a function of m where

$$m = -\frac{1}{C_w^2}\left(\frac{\rho_1}{\rho_w}\right)^2 \frac{\rho_1 \delta_2^2}{\mu_w} \frac{du_1}{dx} \tag{41}$$

by Equations (36) and (37).

To aid the solution of Equation (28) for δ_2, it is convenient to take a linear relation between l and m, *i.e.*,

$$l = f_1 - f_2 m \tag{42}$$

where f_1 and f_2 are constants, in which case Equations (40a) and (41) yield

$$\tfrac{1}{2}c_f = C_w f_1 \frac{\rho_w}{\rho_1} \frac{\mu_w}{\rho_1 u_1 \delta_2} + \frac{f_2}{C_w} \frac{\rho_1}{\rho_w} \frac{\delta_2}{u_1} \frac{du_1}{dx}. \tag{43}$$

We now re-write Equation (43) in a form analogous to Equation (33) for $\mathcal{H}$, *i.e.*, in the second term on the right-hand side we replace ρ_1/ρ_w by T_w/T_1 and, making use of Equations (32) and (34), obtain

$$\tfrac{1}{2}c_f = C_w f_1 \frac{\rho_w}{\rho_1} \frac{\mu_w}{\rho_1 u_1 \delta_2} + \frac{f_2}{C_w} \frac{T_w}{T_r} \delta_2 \left\{\frac{1}{u_1}\frac{du_1}{dx} + \frac{\gamma - 1}{2} Pr^{1/2} \frac{M_1^2}{u_1}\frac{du_1}{dx}\right\}. \tag{44}$$

4. *Solution of the Momentum Integral Equation for* δ_2. Substituting from Equations (33b) and (44) in the momentum integral Equation (28), and making use of the fact that

$$\frac{M_1^2}{u_1}\frac{du_1}{dx} = -\frac{1}{\rho_1}\frac{d\rho_1}{dx}$$

(which follows from Equation (29) and the fact that $dp/d\rho = a^2$) we obtain

$$\frac{d\delta_2}{dx} + G_1 \frac{\delta_2}{u_1}\frac{du_1}{dx} + G_2 \frac{\delta_2}{\rho_1}\frac{d\rho_1}{dx} = C_w f_1 \frac{\rho_w}{\rho_1} \frac{\mu_w}{\rho_1 u_1 \delta_2} \tag{45}$$

where

$$\left.\begin{aligned} G_1 &= 2 + \mathcal{H}_i(1-A) + \left(A\mathcal{H}_i - \frac{f_2}{C_w}\right)\frac{T_w}{T_r} \\ G_2 &= 1 - Pr^{1/2}\frac{\gamma-1}{2}B - Pr^{1/2}\frac{\gamma-1}{2}\left(A\mathcal{H}_i - \frac{f_2}{C_w}\right)\frac{T_w}{T_r}. \end{aligned}\right\} \tag{46}$$

With the assumptions already made, G_1 and G_2 are constants, so that Equation (45) becomes

$$\frac{d}{dx}(\delta_2{}^2 \rho_1{}^{2G\,2} u_1{}^{2G\,1}) = 2C_w f_1 \mu_w \frac{\rho_w}{\rho_1} \rho_1{}^{(2G\,2)-1} u_1{}^{(2G\,1)-1}$$

which integrates to give

$$\delta_2{}^2 = 2C_w f_1 \mu_w \rho_1{}^{(-2G\,2)} u_1{}^{(-2G\,1)} \int_0^x \frac{\rho_w}{\rho_1} \rho_1{}^{(2G\,2)-1} u_1{}^{(2G\,1)-1}\, dx \qquad (47)$$

(where we have assumed that $\mu_w = \mu_w(T_w)$ can be treated as a constant).

Note, that in this integration, $\rho_1{}^{2G\,2} u_1{}^{2G\,1} \delta_2{}^2 = 0$ at $x = 0$, in all cases, including that of the similar solutions with negative index.

Alternatively we have, from Equation (47)

$$R_{\delta\,2}{}^2 = \left(\frac{\rho_1 u_1 \delta_2}{\mu_1}\right)^2$$

$$= 2C_1 f_1 R_X \qquad (48)$$

where

$$R_X = \frac{\rho_1 u_1 X}{\mu_1}$$

with

$$X = \frac{\displaystyle\int_0^x \frac{\rho_w}{\rho_1} \rho_1{}^{(2G\,2)-1} u_1{}^{(2G\,1)-1}\, dx}{\displaystyle\frac{\rho_w}{\rho_1} \rho_1{}^{(2G\,2)-1} u_1{}^{(2G\,1)-1}}. \qquad (49)$$

When evaluating X from Equation (49), it is convenient to replace density by temperature and relate the latter to reference conditions, which we shall denote by suffix 'a'.

Now

$$\frac{\rho_w}{\rho_1} = \frac{T_1}{T_w} = \frac{T_a}{T_w}\frac{T_1}{T_a}$$

and we shall take T_a/T_w as constant*.

If we stipulate now that local conditions outside the boundary layer are reached by an isentropic flow process from the reference conditions (*e.g.*, the reference may be stagnation conditions *behind* a bow shock wave), then

$$\frac{\rho_1}{\rho_a} = \left(\frac{T_1}{T_a}\right)^{1/(\gamma-1)}$$

$$= \left(\frac{T_1}{T_a}\right)^{2\cdot5} \text{ for } \gamma = 1\cdot4\,.$$

With these substitutions we obtain

$$X = \frac{\displaystyle\int_0^x \left(\frac{T_1}{T_a}\right)^{(5G\,2)-1\cdot5} u_1{}^{(2G\,1)-1}\, dx}{\displaystyle\left(\frac{T_1}{T_a}\right)^{(5G\,2)-1\cdot5} u_1{}^{(2G\,1)-1}}. \qquad (50)$$

---

* Strictly, since we have assumed already that T_w/T_r is constant, then, unless $Pr = 1$ when $T_r = T_0 =$ constant, T_a/T_w will vary to some extent along the length of the body. However, errors in X arising from this source should be small.

Equations (48) and (50) give the required solution of the momentum equation, the values of G_1 and G_2 being given by Equations (46). In these, A and B are known as functions of Prandtl number, a suitable value of C_w must be determined in accordance with Equation (38), and we are left with the job of choosing suitable values of f_1, f_2 and $\mathscr{H}_i$.

Now

$$l = f_1 - f_2 m \tag{42}$$

where

$$c_f R_{\delta 2} = 2C_1 l \tag{40b}$$

and consideration of the incompressible flow correlation of Thwaites[6] suggests taking

$$f_1 = 0\cdot 22$$

$$f_2 = 1\cdot 64$$

which give agreement with (a) stagnation point flow and (b) flat-plate (zero pressure gradient) flow.

The choice of $\mathscr{H}_i$ is more difficult, but if we take $\mathscr{H}_i = 2\cdot 6$, as for a flat plate, then we would obtain close agreement with the simplest solution of the incompressible flow momentum equation described by Thwaites in Ref. 6. Alternatively, $\mathscr{H}_i = 2\cdot 4$ (mean between stagnation point and flat-plate values) would give equally good agreement with results (incompressible) for favourable pressure gradients.

Taking the former value of $\mathscr{H}_i$ (2·6), together with the values for f_1 and f_2, we obtain (after rounding off to one place of decimals)

$$\left.\begin{aligned} G_1 &= 4\cdot 6 - 2\cdot 6A + \left(2\cdot 6A - \frac{1\cdot 6}{C_w}\right)\frac{T_w}{T_r} \\ G_2 &= \left(1 - 0\cdot 2Pr^{1/2}B\right) - 0\cdot 2Pr^{1/2}\left(2\cdot 6A - \frac{1\cdot 6}{C_w}\right)\frac{T_w}{T_r}. \end{aligned}\right\} \tag{51a}$$

5. *Results for Pr = 1, μ ∝ T, and Summary of Method.* In this case, $A = B = C_w = 1$ and

$$\left.\begin{aligned} G_1 &= 2 + \frac{T_w}{T_0} \\ G_2 &= 0\cdot 8 - 0\cdot 2\frac{T_w}{T_0} \end{aligned}\right\} \tag{51b}$$

where $T_r = T_0$ is the total temperature.

The indices in Equation (50) are then

$$\begin{aligned} 2G_1 - 1 &= g_1 \text{ (say)} \\ &= 3 + 2\frac{T_w}{T_0} \\ 5G_2 - 1\cdot 5 &= g_2 \text{ (say)} \\ &= 2\cdot 5 - \frac{T_w}{T_0}. \end{aligned}$$

The solution of the momentum equation and determination of c_f then proceeds as follows.

(1) Evaluate X from Equation (50), *i.e.*,

$$X = \frac{\int_0^x \left(\frac{T_1}{T_a}\right)^{g\,2} u_1^{g\,1}\,dx}{\left(\frac{T_1}{T_2}\right)^{g\,2} u_1^{g\,1}}.$$

Alternatively, if M_1 is specified and not u_1, then it is easily shown that

$$X = \frac{\int_0^x \left(\frac{T_1}{T_a}\right)^{4} M_1^{g\,1}\,dx}{\left(\frac{T_1}{T_a}\right)^{4} M_1^{g\,1}}.$$

(Note:—if $Pr = 1$, then the index of (T_1/T_a) is 4, no matter what the value of C_w.)

(2) Immediately, we have (Equation (48))

$$R_{\delta\,2}{}^2 = 0\cdot 44 R_X$$

where

$$R_{\delta\,2} = \frac{\rho_1 u_1 \delta_2}{\mu_1}$$

$$R_X = \frac{\rho_1 u_1 X}{\mu_1}$$

{or $\qquad R_{\delta\,2} = 0\cdot 644 R_X{}^{1/2}$}.

(3) From Equation (41), and the relation between δ_2 and x,

$$m = \left(\frac{\rho_1}{\rho_w}\right)^2 \frac{\rho_1 \delta_2{}^2}{\mu_w} \frac{du_1}{dx}$$

$$= -\,0\cdot 44 \frac{T_w}{T_1} \frac{X}{u_1} \frac{du_1}{dx}$$

or

$$= -\,0\cdot 44 \frac{T_w}{T_0} \frac{X}{M_1} \frac{dM_1}{dx}.$$

(4) Finally, from Equation (40b)

$$c_f R_{\delta\,2} = 2l$$

where l is obtained from m via known correlations, which, if pressure gradients are favourable, may be approximated by

$$l = 0\cdot 22 - 1\cdot 64m.$$

Alternatively, from step 2

$$c_f R_X{}^{1/2} = \frac{2l}{0\cdot 664}$$

$$= 0\cdot 664 \left(\frac{l}{0\cdot 22}\right).$$

6. *Bodies of Revolution.* The method is applicable also to bodies of revolution provided that at each station along the body, the boundary-layer thickness is small compared with the local radius of curvature. The only difference from the two-dimensional case arises in the calculation of X, which is now given by

$$X = \frac{\int_0^x \left(\frac{T_1}{T_a}\right)^{g\,2} u_1^{g\,1} r_0^2 \, dx}{\left(\frac{T_1}{T_a}\right)^{g\,2} u_1^{g\,1} r_0^2}$$

(with a corresponding equation in terms of M_1), where $r_0 = r_0(x)$ is the equation of the generating curve of the body.

TABLE 1

Values of the index g_1 for $Pr = 1$ and $\mu \propto T$.

(Derived from Cohen and Reshotko's transformed similar solutions)

(*a*) From tabulated values

$\frac{T_w}{T_0}$	m	g_1
1	0·0681	4·60
	0·0487	4·47
	(0)	(4·35)
	−0·0602	4·31
	−0·0829	4·31
	−0·1002	4·14
	−0·1064	4·14
0·6	0·0536	4·13
	0·0496	4·01
	0·0369	3·85
	(0)	(3·68)
	−0·0433	3·09
	−0·1040	2·54
0·2	0·0252	3·60
	0·0242	3·52
	0·0203	3·34
	0·0710	2·89
	(0)	(2·68)
	−0·0167	2·26
	−0·0402	1·86
	−0·0504	1·75
2·0	0·0835	5·90
	0·0588	6·06
	−0·0668	7·52
	−0·0751	8·72
	−0·0622	13·15
	−0·0371	23·4
	−0·0179	49·2

(*b*) By graphical interpolation

$\frac{T_w}{T_0}$	m	g_1
0·8	0·04	4·17
	0	4·08
	−0·04	3·72
	−0·08	3·47
0·4	0·02	3·39
	0	3·19
	−0·02	2·83
	−0·04	2·52
	−0·06	2·28
0·1	0·01	3·10
	0·005	2·75
	0	2·45
	−0·005	2·22
	−0·010	2·03
	−0·015	1·86
	−0·020	1·75
	−0·025	1·67
0·05	0·0050	2·98
	0·0025	2·64
	0	2·34
	−0·0025	2·12
	−0·0050	1·96
	−0·0075	1·81
	−0·0100	1·70
	−0·0125	1·63

TABLE 2

2nd Approximation to Transformed Similar Solutions

		1st Approximation			2nd Approximation						Cohen and Reshotko	
$\frac{T_w}{T_0}$	β_i	$g_1 - 1$	$2 + \beta_i(g_1 - 1)$	m	$g_1 - 1$	$2 + \beta_i(g_1 - 1)$	z	m	$\left(\frac{l}{0 \cdot 22}\right)$	f_w''	z	f_w''
0·2	−0·325	2·4	1·22	0·023	2·5	1·19	0·61	0·024	0·386	0·14	0·61	0·14
	−0·30		1·28	0·021	2·4	1·28	0·59	0·021	0·523	0·20	0·58	0·21
	−0·14		1·66	0·0075	1·9	1·73	0·51	0·007	0·841	0·37	0·50	0·38
	0·50		3·20	−0·014	1·3	2·65	0·41	−0·017	1·127	0·61	0·41	0·66
	1·50		5·60	−0·024	1·1	3·65	0·35	−0·036	1·268	0·81	0·37	0·87
	2·00		6·80	−0·026	1·1	4·20	0·33	−0·042	1·313	0·89	0·36	0·95
2·0	−0·1295	6·0	1·22	0·093	(4·9)	1·36	0·57	0·084	0	0	0·57	0
	−0·10		1·40	0·063	5·0	1·50	0·54	0·059	0·44	0·18	0·54	0·18
	0·30		3·80	−0·069	6·5	3·95	0·33	−0·067	1·50	0·99	0·33	0·98
	0·50		5·00	−0·088	(6·5)	5·25	0·29	−0·084	1·63	1·24	0·27	1·24
	1·00		8·00	−0·110	(6·5)	8·5	0·23	−0·103	1·76	1·71	0·18	1·74

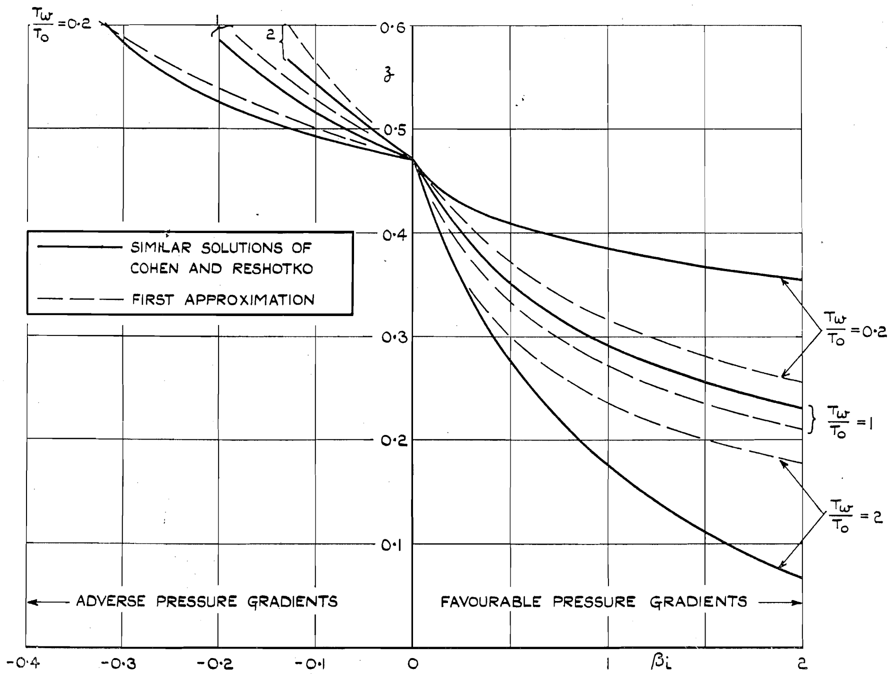

FIG. 1. Comparison of momentum-thickness parameter with results from transformed similar solutions (Cohen and Reshotko).

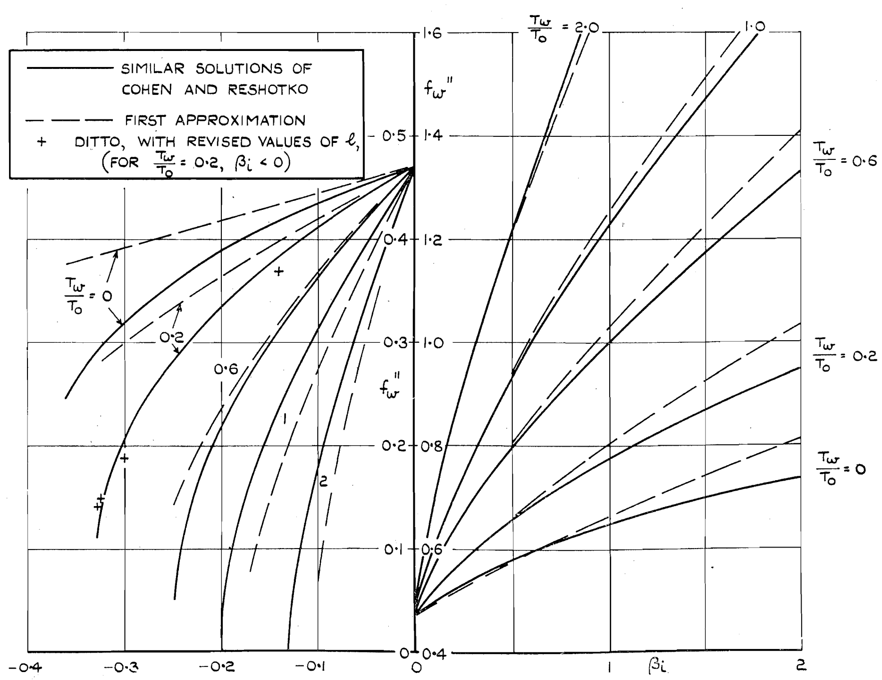

FIG. 2. Comparison of skin-friction parameter with results from transformed similar solutions (Cohen and Reshotko).

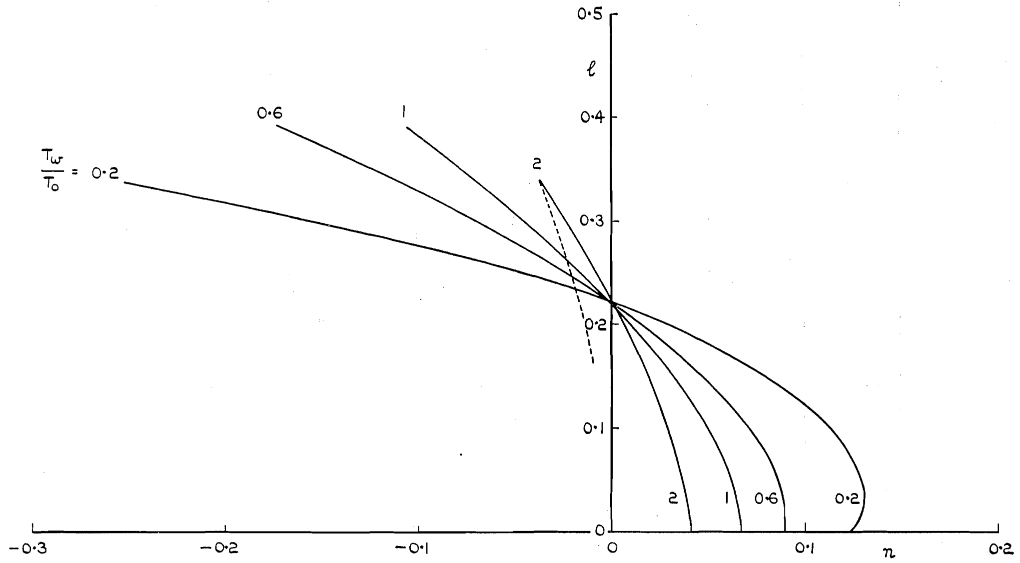

FIG. 3. Skin-friction parameter l plotted against n (both from Cohen and Reshotko[3]).

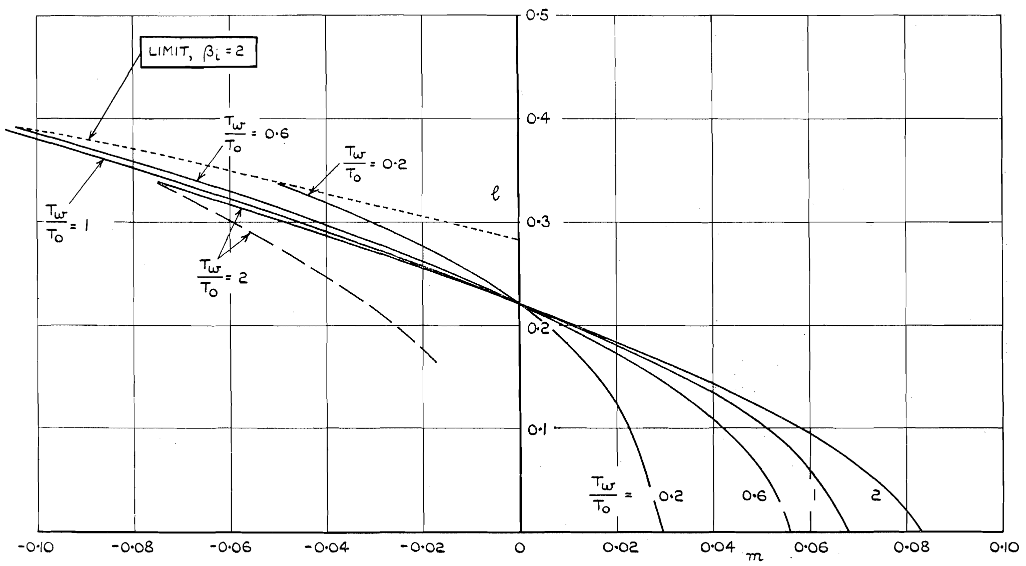

FIG. 4. Skin-friction parameter l, from Cohen and Reshotko[3], plotted against the parameter m of the present method.

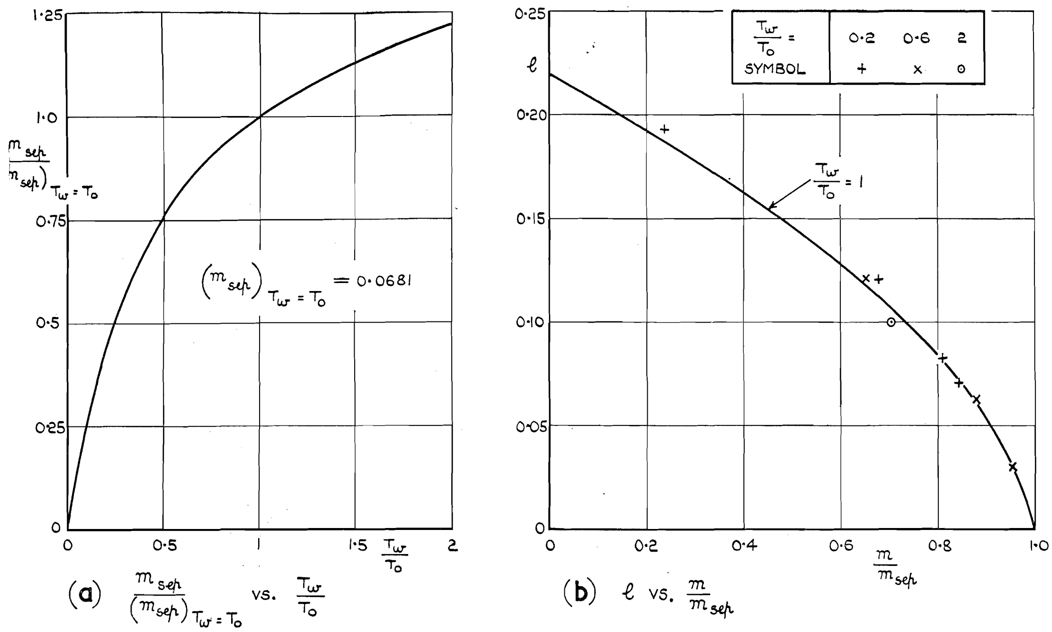

FIG. 5. Reduction of curves of l against m for adverse pressure gradients ($m > 0$).

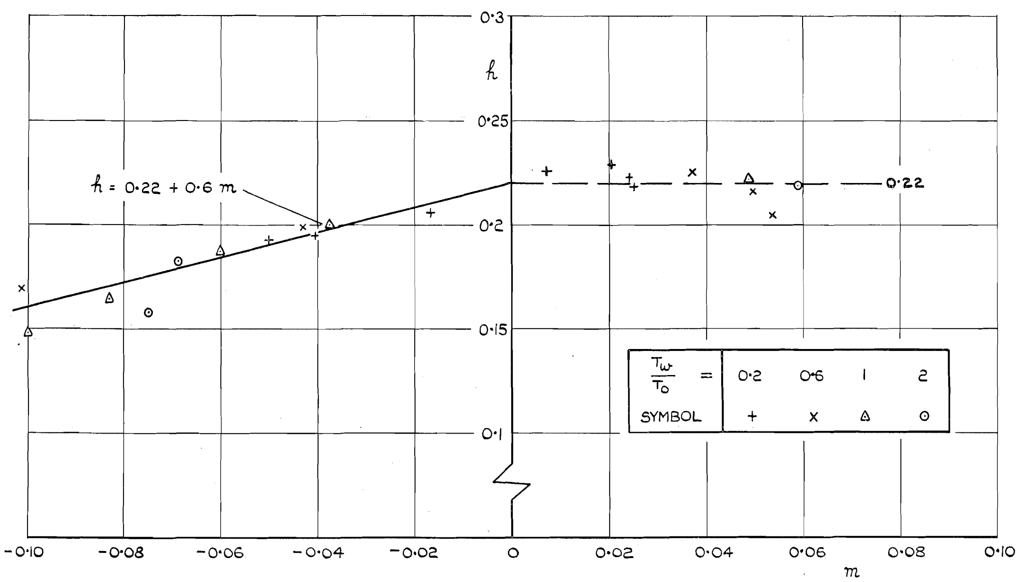

FIG. 6. Variation of heat-transfer parameter h, with m. (Values derived from Cohen and Reshotko[3].)

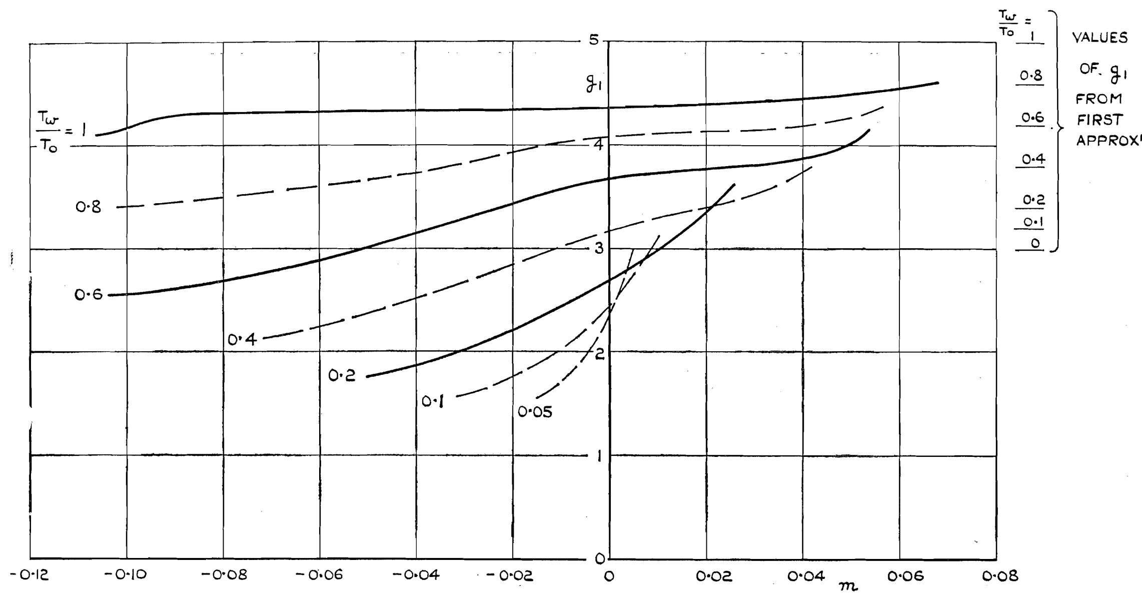

FIG. 7. Values of the index g_1 derived from Cohen and Reshotko's similar solutions.

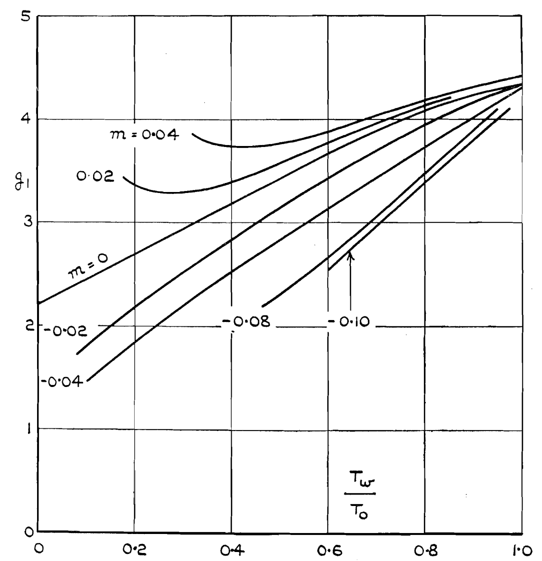

FIG. 8. Variation of g_1 with T_w/T_0 at constant m.

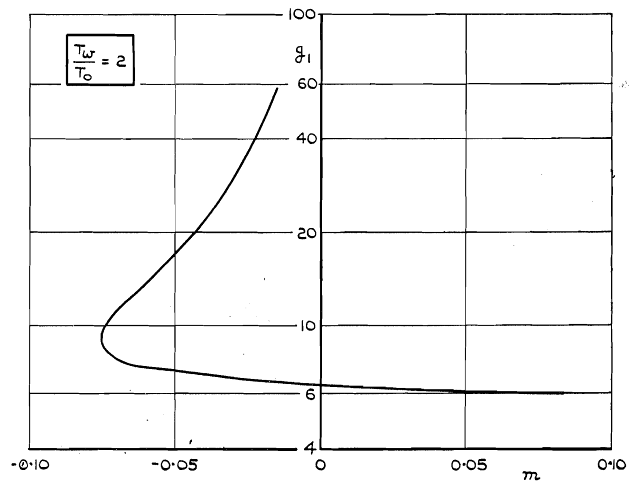

FIG. 9. Values of g_1 for $T_w/T_0 = 2$.

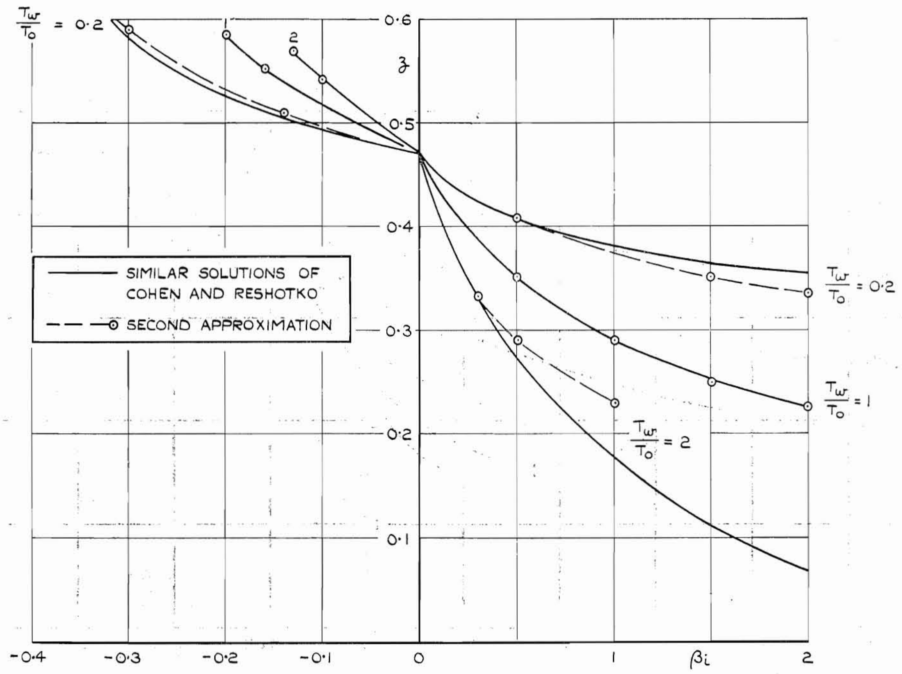

FIG. 10. Comparison of second approximation to momentum-thickness parameter with results from Cohen and Reshotko. (Compare with Fig. 1.)

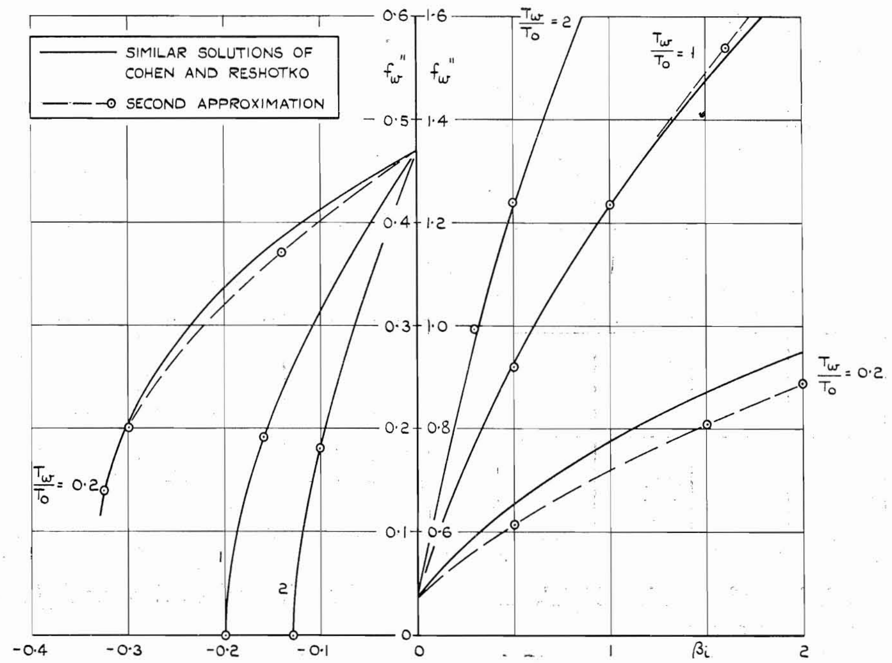

FIG. 11. Comparison of second approximation to skin-friction parameter with results from Cohen and Reshotko. (Compare with Fig. 2.)

(8247) Wt. 66/999 K.5 11/61 Hw.

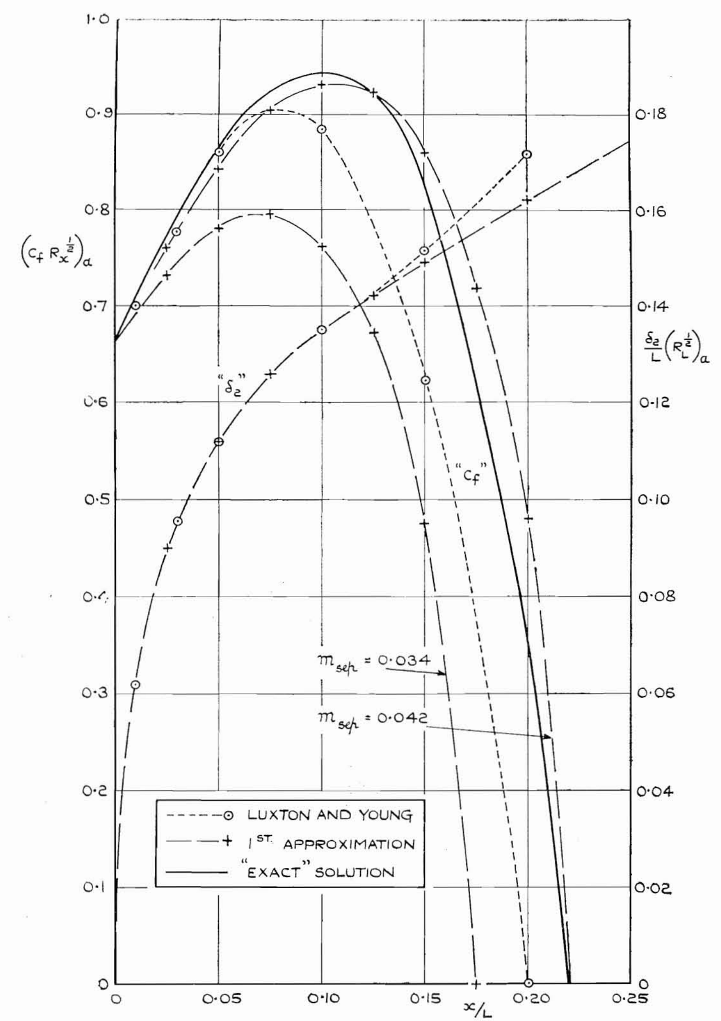

FIG. 12. Comparison of results for the case $u_1 = u_a \cdot (1 - x/L)$, $M_a = 4$, $T_w = T_a$ ($Pr = 1$, $\mu \propto T$).

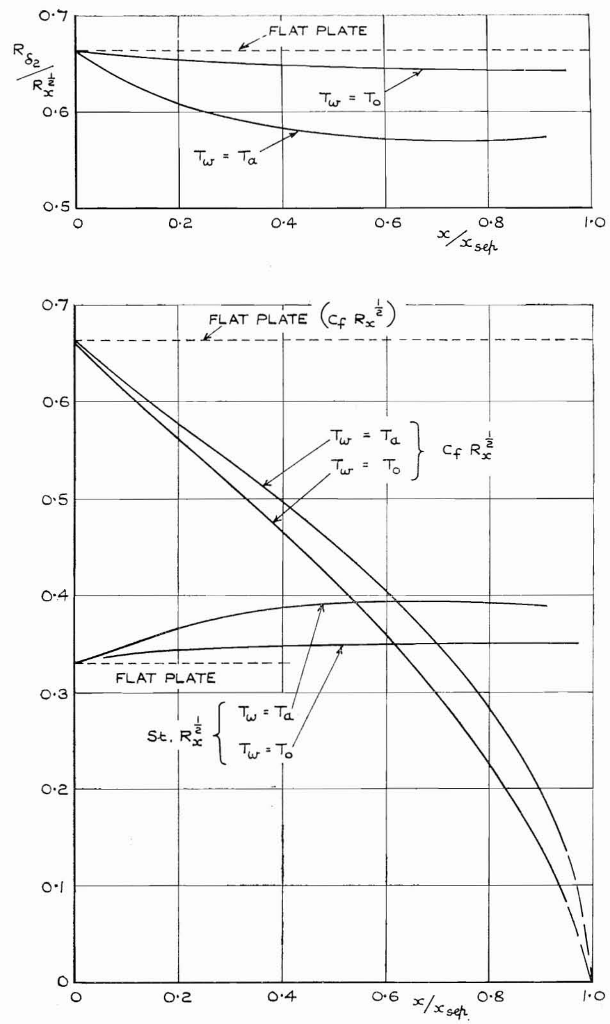

FIG. 13. Values of $R_{\delta 2}$, C_f and St, based on local conditions for $u_1 = u_a (1 - x/L)$, $M_a = 4$ ($Pr = 1$ $\mu \propto T$).

R. & M. 3218 533.6.011.6:
R. J. Monaghan 532.526.2
May, 1960

EFFECTS OF HEAT TRANSFER ON LAMINAR BOUNDARY-LAYER DEVELOPMENT UNDER PRESSURE GRADIENTS IN COMPRESSIBLE FLOW

An approximate analysis, outlined in the Appendix, shows that momentum thickness, skin friction and heat transfer of the compressible laminar boundary layer developing under pressure gradients may be given by formulae formally the same as those obtaining under zero pressure gradient conditions if an appropriate length transformation is applied to the x-co-ordinate. Also, the formulae for skin friction and heat transfer include factors l and h respectively, which are functions of a pressure gradient parameter m.

P.T.O.

R. & M. 3218 533.6.011.6:
R. J. Monaghan 532.526.2
May, 1960

EFFECTS OF HEAT TRANSFER ON LAMINAR BOUNDARY-LAYER DEVELOPMENT UNDER PRESSURE GRADIENTS IN COMPRESSIBLE FLOW

An approximate analysis, outlined in the Appendix, shows that momentum thickness, skin friction and heat transfer of the compressible laminar boundary layer developing under pressure gradients may be given by formulae formally the same as those obtaining under zero pressure gradient conditions if an appropriate length transformation is applied to the x-co-ordinate. Also, the formulae for skin friction and heat transfer include factors l and h respectively, which are functions of a pressure gradient parameter m.

P.T.O.

R. & M. 3218 533.6.011.6:
R. J. Monaghan 532.526.2
May, 1960

EFFECTS OF HEAT TRANSFER ON LAMINAR BOUNDARY-LAYER DEVELOPMENT UNDER PRESSURE GRADIENTS IN COMPRESSIBLE FLOW

An approximate analysis, outlined in the Appendix, shows that momentum thickness, skin friction and heat transfer of the compressible laminar boundary layer developing under pressure gradients may be given by formulae formally the same as those obtaining under zero pressure gradient conditions if an appropriate length transformation is applied to the x-co-ordinate. Also, the formulae for skin friction and heat transfer include factors l and h respectively, which are functions of a pressure gradient parameter m.

P.T.O.

R. & M. 3218 533.6.011.6:
R. J. Monaghan 532.526.2
May, 1960

EFFECTS OF HEAT TRANSFER ON LAMINAR BOUNDARY-LAYER DEVELOPMENT UNDER PRESSURE GRADIENTS IN COMPRESSIBLE FLOW

An approximate analysis, outlined in the Appendix, shows that momentum thickness, skin friction and heat transfer of the compressible laminar boundary layer developing under pressure gradients may be given by formulae formally the same as those obtaining under zero pressure gradient conditions if an appropriate length transformation is applied to the x-co-ordinate. Also, the formulae for skin friction and heat transfer include factors l and h respectively, which are functions of a pressure gradient parameter m.

P.T.O.

Cohen and Reshotko's transformed similar solutions are used to provide values of $l(m)$ and $h(m)$ and of an index appearing in the length transformation. Compared with the pressure gradient parameter n of Cohen and Reshotko's generalised method, the present parameter $m = \frac{T_w}{T_0} n$ (where T_w is surface and T_0 is stagnation temperature), and there is a good collapse of values of l and h when plotted against m.

If pressure gradients are adverse, then the value of m at natural separation (which depends on T_w/T_0) is an additional parameter in the determination of the skin-friction parameter l, but h is approximately a constant, equal to its zero pressure gradient value, in this region.

Comparisons are made also for an external velocity variation $u_1 = u_a (1 - x)$.

Cohen and Reshotko's transformed similar solutions are used to provide values of $l(m)$ and $h(m)$ and of an index appearing in the length transformation. Compared with the pressure gradient parameter n of Cohen and Reshotko's generalised method, the present parameter $m = \frac{T_w}{T_0} n$ (where T_w is surface and T_0 is stagnation temperature), and there is a good collapse of values of l and h when plotted against m.

If pressure gradients are adverse, then the value of m at natural separation (which depends on T_w/T_0) is an additional parameter in the determination of the skin-friction parameter l, but h is approximately a constant, equal to its zero pressure gradient value, in this region.

Comparisons are made also for an external velocity variation $u_1 = u_a (1 - x)$.

Cohen and Reshotko's transformed similar solutions are used to provide values of $l(m)$ and $h(m)$ and of an index appearing in the length transformation. Compared with the pressure gradient parameter n of Cohen and Reshotko's generalised method, the present parameter $m = \frac{T_w}{T_0} n$ (where T_w is surface and T_0 is stagnation temperature), and there is a good collapse of values of l and h when plotted against m.

If pressure gradients are adverse, then the value of m at natural separation (which depends on T_w/T_0) is an additional parameter in the determination of the skin-friction parameter l, but h is approximately a constant, equal to its zero pressure gradient value, in this region.

Comparisons are made also for an external velocity variation $u_1 = u_a (1 - x)$.

Cohen and Reshotko's transformed similar solutions are used to provide values of $l(m)$ and $h(m)$ and of an index appearing in the length transformation. Compared with the pressure gradient parameter n of Cohen and Reshotko's generalised method, the present parameter $m = \frac{T_w}{T_0} n$ (where T_w is surface and T_0 is stagnation temperature), and there is a good collapse of values of l and h when plotted against m.

If pressure gradients are adverse, then the value of m at natural separation (which depends on T_w/T_0) is an additional parameter in the determination of the skin-friction parameter l, but h is approximately a constant, equal to its zero pressure gradient value, in this region.

Comparisons are made also for an external velocity variation $u_1 = u_a (1 - x)$.

Publications of the Aeronautical Research Council

ANNUAL TECHNICAL REPORTS OF THE AERONAUTICAL RESEARCH COUNCIL (BOUND VOLUMES)

1941 Aero and Hydrodynamics, Aerofoils, Airscrews, Engines, Flutter, Stability and Control, Structures. 63*s.* (post 2*s.* 3*d.*)

1942 Vol. I. Aero and Hydrodynamics, Aerofoils, Airscrews, Engines. 75*s.* (post 2*s.* 3*d.*)
Vol. II. Noise, Parachutes, Stability and Control, Structures, Vibration, Wind Tunnels. 47*s.* 6*d.* (post 1*s.* 9*d.*)

1943 Vol. I. Aerodynamics, Aerofoils, Airscrews. 80*s.* (post 2*s.*)
Vol. II. Engines, Flutter, Materials, Parachutes, Performance, Stability and Control, Structures. 90*s.* (post 2*s.* 3*d.*)

1944 Vol. I. Aero and Hydrodynamics, Aerofoils, Aircraft, Airscrews, Controls. 84*s.* (post 2*s.* 6*d.*)
Vol. II. Flutter and Vibration, Materials, Miscellaneous, Navigation, Parachutes, Performance, Plates and Panels, Stability, Structures, Test Equipment, Wind Tunnels. 84*s.* (post 2*s.* 6*d.*)

1945 Vol. I. Aero and Hydrodynamics, Aerofoils. 130*s.* (post 3*s.*)
Vol. II. Aircraft, Airscrews, Controls. 130*s.* (post 3*s.*)
Vol. III. Flutter and Vibration, Instruments, Miscellaneous, Parachutes, Plates and Panels, Propulsion. 130*s.* (post 2*s.* 9*d.*)
Vol. IV. Stability, Structures, Wind Tunnels, Wind Tunnel Technique. 130*s.* (post 2*s.* 9*d.*)

1946 Vol. I. Accidents, Aerodynamics, Aerofoils and Hydrofoils. 168*s.* (post 3*s.* 3*d.*)
Vol. II. Airscrews, Cabin Cooling, Chemical Hazards, Controls, Flames, Flutter, Helicopters, Instruments and Instrumentation, Interference, Jets, Miscellaneous, Parachutes. 168s. (post 2*s.* 9*d.*)
Vol. III. Performance, Propulsion, Seaplanes, Stability, Structures, Wind Tunnels. 168*s.* (post 3*s.*)

1947 Vol. I. Aerodynamics, Aerofoils, Aircraft. 168*s.* (post 3*s.* 3*d.*)
Vol. II. Airscrews and Rotors, Controls, Flutter, Materials, Miscellaneous, Parachutes, Propulsion, Seaplanes, Stability, Structures, Take-off and Landing. 168*s.* (post 3*s.* 3*d.*)

Special Volumes

Vol. I. Aero and Hydrodynamics, Aerofoils, Controls, Flutter, Kites, Parachutes, Performance, Propulsion, Stability. 126*s.* (post 2*s.* 6*d.*)
Vol. II. Aero and Hydrodynamics, Aerofoils, Airscrews, Controls, Flutter, Materials, Miscellaneous, Parachutes, Propulsion, Stability, Structures. 147*s.* (post 2*s.* 6*d.*)
Vol. III. Aero and Hydrodynamics, Aerofoils, Airscrews, Controls, Flutter, Kites, Miscellaneous, Parachutes, Propulsion, Seaplanes, Stability, Structures, Test Equipment. 189*s.* (post 3*s.* 3*d.*)

Reviews of the Aeronautical Research Council

1939–48 3*s.* (post 5*d.*) 1949–54 5*s.* (post 5*d.*)

Index to all Reports and Memoranda published in the Annual Technical Reports

1909–1947 R. & M. 2600 6*s.* (post 2*d.*)

Indexes to the Reports and Memoranda of the Aeronautical Research Council

Between Nos. 2351–2449	R. & M. No. 2450	2*s.* (post 2*d.*)
Between Nos. 2451–2549	R. & M. No. 2550	2*s.* 6*d.* (post 2*d.*)
Between Nos. 2551–2649	R. & M. No. 2650	2*s.* 6*d.* (post 2*d.*)
Between Nos. 2651–2749	R. & M. No. 2750	2*s.* 6*d.* (post 2*d.*)
Between Nos. 2751–2849	R. & M. No. 2850	2*s.* 6*d.* (post 2*d.*)
Between Nos. 2851–2949	R. & M. No. 2950	3*s.* (post 2*d.*)
Between Nos. 2951–3049	R. & M. No. 3050	3*s.* 6*d.* (post 2*d.*)

HER MAJESTY'S STATIONERY OFFICE

from the addresses overleaf

R. & M. No. 3218

Printed and published by
HER MAJESTY'S STATIONERY OFFICE

To be purchased from
York House, Kingsway, London W.C.2
423 Oxford Street, London W.1
13A Castle Street, Edinburgh 2
109 St. Mary Street, Cardiff
39 King Street, Manchester 2
50 Fairfax Street, Bristol 1
2 Edmund Street, Birmingham 3
80 Chichester Street, Belfast 1
or through any bookseller

Printed in England

R. & M. No. 3218

S.O. Code No. 23-3218